MULTISENSORY EXPECTATIONS SHAPE OLFACTORY INPUT TO THE BRAIN

By

LINDSEY CZARNECKI

A dissertation submitted to the

Graduate School-New Brunswick

Rutgers, The State University of New Jersey

In partial fulfillment of the requirements

For the degree of

Doctor of Philosophy

Graduate Program in Psychology

Written under the direction of

John P. McGann

And approved by

_____

_____

_____

_____

New Brunswick, New Jersey

January 2017

ABSTRACT OF THE DISSERTATION

Multisensory expectations shape olfactory input to the brain

by LINDSEY CZARNECKI

Dissertation Director:
John McGann

Mammals spontaneously learn contingencies among sensory stimuli including across sensory modalities. Stimulus recognition is faster and more accurate when cross-modal cues are congruent with previous experience (e.g. Gottfried & Dolan, 2003). This suggests that information from multiple sensory modalities could converge in early sensory processing regions in the brain. In the olfactory system, the olfactory bulb glomerulus receives heavy anatomical ñtop-downò projections from brain regions that might contain such information. Using wide-field *in vivo* imaging of awake head-fixed mice expressing the calcium indicator GCaMP in GABAergic periglomerular (PG) interneurons in the olfactory bulb, neural activity can be evoked not only by odors but also by lights, tones, and whisker deflections. Anesthesia eliminates responses to non-olfactory stimuli and tracheotomy demonstrates that these signals are not driven by respiratory changes. Non-olfactory stimuli were most effective when presented at long inter-stimulus intervals (e.g. > 60 sec), but evoked observable bulbar activity at all intervals tested. To test whether non-olfactory stimuli convey odor-predictive information to the olfactory system, mice were presented with 13 presentations of a light-

tone-odor sequence to establish an expectation about the odor. This expectation was subsequently violated by omitting the expected tone while presenting the light and odor as usual. There was an increase in GABAergic interneuron activity during the odor presentation when its preceding tone cue was omitted. Because these interneurons are responsible for presynaptic inhibition of olfactory sensory neurons (OSNs), the primary sensory neurons of the olfactory system, the experiment was repeated in separate animals expressing the exocytosis indicator synaptopHluorin (spH) in OSNs. This revealed a complementary suppression of odorant-evoked neurotransmitter release from OSNs during the odorant presentation in which the tone was unexpectedly omitted. This effect was not observed if mice were anesthetized or if the absence of the tone was unsurprising. Imaging of sniff-by-sniff calcium dynamics in OSN presynaptic terminals revealed that suppression of activity is present on the first inhalation of odorant during the surprising trial. This reduction in presynaptic calcium suggested a $GABA_B$ receptor-mediated presynaptic inhibition. Blocking $GABA_B$ receptors with CGP35348 abolished the effect of tone omission on odorant-evoked neurotransmitter release. To test whether PG interneurons are sensitive to olfactory expectations in the absence of bottom-up odor information, mice were again presented with the light-tone-odor sequence, but the odor was subsequently omitted. On this odor-omitted trial, the magnitude of GCaMP signals during the time of the expected odor presentation was not significantly different from the previous odor-present trial, but the spatial pattern of activity was diffuse and not obviously glomerular. In a modified paradigm, two different tones were presented with two different odors, with each pairing delivered on 13 interleaved trials. When the odor was then switched such that the tone was unexpectedly followed by the other odorant, the

amplitudes of the odor-evoked responses became more similar to each other. These experiments show that non-olfactory stimuli can drive activity in the olfactory bulb and that expectations and violations thereof can shape sensory processing as early as the primary input into the brain.

ACKNOWLEDGEMENTS

This dissertation research has infinitely interested me and I am so grateful to have been able to ask these questions. I would like to thank my mentor, Dr. John McGann for allowing me to tackle these topics that I find so fascinating. I would also like to thank him for the training I received throughout the entire PhD process. This mentorship began early, when on my first day when he told me, ñto be a neuroscientist, you must first be an electricianò and I saw the ins and outs of building a new laboratory. This was invaluable insight I will always appreciate throughout my career.

I am grateful for the guidance I have received from my dissertation committee members; Dr. Charles Gallistel, Dr. David Vicario, and Dr. David Margolis. I have benefited from their knowledge both through this committee and in numerous classes, conferences, and talks that have shaped my graduate experience.

I have been lucky enough to spend my PhD training in a wonderfully productive and supportive environment. I have benefited from so many conversations with fellow lab members, graduate students, and faculty. I would like to thank the members of the McGann Lab for their hard work and dedication. I particularly owe my sincerest gratitude to Marley Kass and Michelle Rosenthal for their years of encouragement and friendship.

Lastly, I would like to thank my family and friends who have been boundlessly encouraging and supportive.

TABLE OF CONTENTS

LIST OF ILLUSTRATIONS

1. Introduction

Traditional models of sensory processing presume that peripheral sensory organs furnish the brain with raw information about the world that is then analyzed and interpreted by a hierarchy of subcortical and cortical structures. These higher structures are increasingly understood to learn statistical regularities in the sensory input stream, essentially building a cognitive representation of the contingencies among stimuli in the outside world. Behaviorally, learning stimulus patterns and having well informed expectations serves to more accurately filter irrelevant information, enhance signal detection, and generally foster rapid behavioral responses (Gottfried & Dolan, 2003; Henderson & Hollingworth, 1999) and decision making (Mitchell et al., 1995). Conversely, violating expectations by changing or omitting an expected stimulus produces dramatic changes in neurosensory processing, delays behavioral responding and decreases task accuracy (Gottfried & Dolan, 2003). Physiological correlates of these cognitive models have been observed in the cerebral cortex (Gottfried & Dolan, 2003; Shulman et al., 1997; de Araujo et al., 2005), but the sensory consequences of expectation confirmation and violation suggest that these cognitive influences might shape earlier sensory processing. Using optical neurophysiology in a mouse model, this dissertation will demonstrate that in the mouse olfactory system, top-down multimodal and non-olfactory sensory information reaches all the way to the first neurons in the brainôs olfactory circuit and that establishing and violating expectations can actually modulate the synaptic terminals of primary sensory neurons at the input to the brain.

1.1: Expectations and learning modulate percepts and sensory neurophysiology

Perceptual experiments in multiple sensory modalities have shown that context and expectations about a stimulus can change reports of stimulus quality (Morrot et al., 2001; Herz & von Clef, 2001), strength (Dalton, 1996; Zellner & Kautz, 1990; Zellner & Whitten, 1999), alter speed of responding, and modulate response accuracy (Gottfried & Dolan, 2003; Zelano et al., 2011). fMRI data shows that early visual areas such as primary visual cortex are indeed task-dependently modulated (Bar, 2004). It has been hypothesized that when an individual is confronted with an object recognition task, the prefrontal cortex may first generate an expectation based off of quickly extracted low frequency visual information to reduce the realm of possible interpretations of that visual input and subsequently modulate visual sensory cortices (Bar, 2003). While task-dependent metabolic activity increases in early visual areas, blood flow in other sensory areas simultaneously decreases, indicating a prioritization of metabolic resources (Shulman et al., 1997). However, there is reason to think that modulation occurs even earlier than primary sensory cortices.

In the chemical senses, several studies have shown that multimodally-derived expectations and mismatches of sensory cues can alter perception and task accuracy. Darker colored solutions are reported as smelling stronger (Zellner & Kautz, 1990; Zellner & Whitten, 1999), and color appropriateness may also influence concentration perception (Zellner & Whitten, 1999; Zellner & Kautz, 1990). Coloring white wine red influences olfactory descriptions of the wine, with descriptions more closely matching typical perceptions of red wines (Morrot et al., 2001). Color-odor associations alter perception of components in odor mixture (Aro et al., 2012) such that in a binary mixture of equal components, when a color is congruent with a mixture component (yellow-green

with limonene), that odor is perceived as being more dominant in the mixture. This appears to be a perceptual, rather than reporting, effect, because participants do not report the odor associated with the color cue when it is unambiguously wrong (Aro et al., 2012). This also suggests that multimodal stimuli are most effective at evoking perceptual alterations when there is stimulus ambiguity. It appears that coloring liquids induces an expectation of a specific sensory experience and this expectation may drive misidentification or misperception (Spence et al., 2010).

Verbal context is also closely associated with perception and valence ratings. Instructions change reports of odor intensity, but do not differentially affect detection thresholds (Dalton, 1996). Brand labels (Moskowitz, 1979) and labels of odor source, even those which do not match well, (Distel & Hudson, 2001) can increase pleasantness ratings. The same odor (a mixture of isovaleric and butyric acids), tested a week apart, was rated as different in both quality and pleasantness depending on the valence of the label applied (ñparmesan cheeseò or ñvomitò) (Herz & von Clef, 2001). In this case, participants reported different memories and used different descriptors of the odor depending on the applied label. Using lexical context to orient attention towards multiple sensory systems also impacts perceptual reports. Ad copy merely mentioning the presence of multiple senses before chewing gum induced increased reports of positive flavor perception and a more multisensory description of the gum (Elder & Krishna, 2009). However, adding a cognitive load task eliminates the multisensory ad copy-induced enhancement in positive flavor perception. This suggests that cognitive resources are necessary for sensory primes to increase positive sensory reports and points to higher order ñtop-downò mechanisms.

Functional imaging experiments during similar tasks support this claim. Labeling the same odor (isovaleric acid with cheddar cheese flavor) with different names (ñcheddar cheeseò or ñbody odorò) induced different rating of valence, but not intensity with correlated changes in BOLD signal in the medial orbitofrontal cortex (mOFC)/anterior cingulate (ACC), and amygdala. Using the same labels on clean air also influenced pleasantness ratings, but not intensity ratings, with similar albeit weaker corresponding BOLD signal changes in the mOFC/ACC (de Araujo et al., 2005).

Outside of valence changes, in an olfactory search task in which participants were cued to expect one of two different odors and asked to report the identity of the actual odor presented, response accuracy is better and quicker when the cue and the odor are congruent (Zelano et al., 2011). Incredibly, *anticipating* a cued odor induced odor-like cortical activity patterns in the anterior piriform and orbitofrontal cortices. These pre-odor patterns in the anterior piriform cortex correlated both with subsequent odor-evoked activity and behavioral accuracy. That is, the more the anticipatory pattern of activity resembled the odor-evoked activity pattern, the higher the task accuracy. Olfactory detection accuracy and reaction time was also facilitated when visual and olfactory stimuli were more highly congruent (for example, a picture of an orange matched with orange odor). During this task, the left anterior hippocampus and rostromedial OFC were more active in congruent conditions (Gottfried & Dolan, 2003).

1.2: Olfactory system overview

During an inhalation, odorants bind to odor receptors on olfactory sensory neurons (OSNs) in the olfactory epithelium. Each OSN expresses just one out of about 1000 different receptor types (Buck & Axel, 1991). OSNs project their axons from the

olfactory epithelium over the surface of the olfactory bulb (OB) where they segregate and sort themselves such that axons of each receptor type converge into one or two glomeruli (Mombaerts et al., 1996; Fig. 1A). Different odors of varying molecular features bind to subsets of olfactory receptors and in turn drive unique subsets of corresponding olfactory glomeruli, creating a combinatorial code of odor identity (Malnic et al., 1999; Buck, 2004 for review).

The glomerular layer of the olfactory bulb also contains a heterogeneous population of juxtraglomerular cells including periglomerular (PG), short axon (SA), and external tufted (ET) cells (Fig. 1A&B). Subsets of juxtaglomerular cells express glutamic acid decarboxylase (Gad) 65, Gad67, and others are positive for tyrosine hydroxylase (TH; Kosaka et al, 1995; Kosaka & Kosaka, 2008; Shao et al., 2009). $Gad65^+$ PG cells sometimes co-express Gad67, and Gad67 SA cells often co-express TH (Kosaka et al., 1995; Kosaka & Kosaka, 2008). GABAergic periglomerular interneurons are important in $GABA_B$-mediated presynaptic inhibition of OSNs (Keller et al., 1998; Shao et al., 2009; McGann et al., 2005). Of particular interest to the current work are $Gad65^+$ interneurons, which innervate one glomerulus and can cause presynaptic inhibition of OSN synaptic terminals. These PG cells can be driven either directly by ORN input or indirectly by ET cells and subsequently inhibit back onto OSNs (Shao et al., 2009). These neurons are, therefore, capable of shaping the magnitude of synaptic signals composing the primary sensory representation of an incoming odorant.

Short axon cells, despite the name, have wide reaching projections spanning up to 2mm (Aungst et al., 2003). SA cells have two pathways to modulate intrabulbar activity as well as OB output. SA cell activity can induce GABA-ergic and dopaminergic

inhibition followed by rebound excitation in ET cells. ET cells in turn can either directly modulate OB output neurons, mitral cells, or modulate output indirectly through PG cells, as mentioned above (Liu et al., 2016). With increasing concentrations of odor, glomeruli tend to be recruited (Johnson & Leon, 2000; Koulakov, Gelperin & Rinberg, 2007). Activity of SA cell activity through this microcircuit could therefore serve to weaken the activity of glomeruli that would not normally respond at ecological concentrations (Liu et al., 2016). Morphologically identified SA cells have also been shown to activate far (several glomeruli away) PG cells (Aungst et al., 2003). These long-range connections in the glomerular layer of the OB could serve to widely distribute information across many glomeruli and potentially shape bottom-up olfactory input globally.

Olfactory bulb projection neurons, mitral and tufted (M/T) cells, have cell bodies in the deeper mitral cell layer and extend dendrites both superficially into glomeruli and laterally to other M/T cells innervating neighboring glomeruli. M/T cells project axons out of the OB, forming the lateral olfactory tract, and send axons to the piriform cortex, anterior olfactory nucleus, and amygdala (Haberly & Prince, 1977; Scalia & Winans, 1975). The external plexiform layer, between the glomerular and mitral cell layers contain additional populations of GABAergic interneurons and synapses of secondary M/T cell dendrites and the apical dendrites of granule cells, with the granule cell layer being the deepest cell layer in the OB (Shepherd, 2004; Hamilton et al., 2005).

Afferent inputs from higher-order areas to the OB are in fact denser than connections originating from the OB to the same areas (Shipley & Ennis, 1996; Shepherd, 2004). Centrifugal fibers have been noted in the olfactory bulb for over one hundred years (Golgi, 1875; Cajal, 1911), but their precise origin, targets, and functions

are still being elucidated. There are neuromodulatory serotonergic inputs from the dorsal raphé (deOlmos et al., 1978; McLean & Shipley, 1987), noradgenergic inputs from locus coeruleus (LC; Devore & Linster, 2012 for review), and cholinergic fibers via the horizontal limb of the diagonal band of Broca (HDB; Prince & Powell, 1970; Devore & Linster, 2012 for review). Other areas such as piriform cortex (PCx) (Heimer, 1968; Scalia & Winans, 1975), anterior olfactory nucleus (AON; Scalia & Winans, 1975, Boyd et al., 2012, Markopolous et al., 2012), olfactory tubercle (Scalia & Winans, 1975), and substantia innominata (Prince & Powell, 1970) also extensively target the main olfactory bulb. Many of these regions have been shown to directly influence the activity of PG cells in the glomerular layer, notably projections from the AON (Markopoulos et al. 2012), raphe (Petzold et al. 2009), and locus coeruleus (Fast & McGann, 2016). It has been hypothesized that these descending systems harness the local inhibitory circuitry of the glomerulus to shape incoming sensory information based on learned information (McGann 2013; McGann 2015; Kass et al. 2013).

If the olfactory bulb receives top-down anatomical connections and behavioral studies show rodents can respond in under 300 ms in an odor discrimination task (Abraham et al., 2004), it stands to reason that primary sensory areas may be privy to sensory expectations, perhaps even those that are derived from non-olfactory senses. Functional consequences of centrifugal projections to the earliest neurons in sensory systems during cognitive engagement in awake animals are largely unknown. Using wide-field fluorescence microscopy in awake, head fixed mice, this dissertation will show such effects in the olfactory bulb glomerulus. The glomerulus is the earliest potential point of convergence between ñbottom-upò incoming sensory stimulation and

ñtop-downò centrifugal input in the olfactory system. Since multimodally derived sensory expectations and decisions occur very rapidly, it is hypothesized that the olfactory bulb may receive information regarding non-olfactory stimuli and sensory representations in the olfactory bulb might be informed by cognitive states at the very first stage in sensory processing. This dissertation aims to 1.) evaluate responses in olfactory bulb periglomerular interneurons to non-olfactory stimuli and 2.) evaluate the consequences of violating multimodally-derived olfactory expectations in periglomerular interneurons as well as olfactory sensory neurons, the first neuron in the sensory system.

2. Materials and Methods

2.1 Subjects

A total of 73 mice were used in these experiments of which 36 were male and 37 were female. All mice were between 2 and 10 months of age the time of experimentation. GCaMP3 (B6;129S-Gt(ROSA)26Sor$^{tm38(CAG-GCaMP3)Hze}$/6 line; Jackson Labs stock number 014538; mixed C57BL/6J and C57BL/6N background (Zariwala et al., 2012)) was expressed in via cre recombinase-mediated excision of a floxed STOP codon in cells expressing cre recombinase from the *gad2* locus (Gad2$^{tm2(cre)Zjh}$/6 Gad2-cre recombinase line; Jackson Labs stock number 010802; mixed 129 and C57BL/6 background (Taniguchi et al., 2011)) after the manner of Wachowiak et al (2013). OMP-spH mice were heterozygous for olfactory marker protein and spH on a mixed albino C57BL/6 and 129 (Czarnecki et al., 2011) background. Wild-type mice for calcium imaging experiments were 129 strain mice to facilitate comparison to the OMP-spH mice. Mice for tracheotomy used calcium indicator GCaMP6 and were an F1 cross of the Gad2$^{tm2(cre)Zjh}$/6 Gad2-cre recombinase line (Jackson Labs stock number 010802; mixed 129 and C57BL/6 background (Taniguchi et al., 2011)) and the B6;129S-

Gt(ROSA)26Sor$^{tm95.1(CAG-GCaMP6\ f)Hze}$/J line (Jackson Labs stock number 024105; mixed C57BL/6J and C57BL/6N background. All mice were maintained on a 12:12 h light:dark cycle and given *ad libitum* food and water. All experiments were conducted in accordance with protocols approved by the Rutgers University Institutional Animal Care and Use Committee.

2.2 Non-Surgical Procedures

2.2.1 Restraint training

All mice underwent 2 to 4 daily 60-minute restraint training sessions in custom restraint tubes prior to surgery. These tubes were ~2.8 cm in diameter and ventilated. Following headcap implantation, some mice received up to two additional 90 minute restraint sessions in which they were secured to a custom headholder via the implanted headcap in a mockup of the imaging apparatus.

2.2.2 Intranasal dye loading

OSNs were loaded with either 4% Calcium Green dextran potassium salt, a dextran-conjugated, fluorescent calcium-sensitive dye (OSN calcium transients in Fig.6A-D, Fig. 7, Fig. 8C & Fig. 10B; Life Technologies, Grand Island, NY) or 10kD AlexaFlur 568-conjugated dextran amine (comparison of GCaMP3 expression to OSN afferents in Fig. 1C; Life Technologies, Grand Island, NY) by intranasal instillation during headcap implantation after the manner of Wachowiak and Cohen (2001) as previously reported (Czarnecki et al., 2011). Briefly, mice were anesthetized with 1000 µg/kg dexmedetomadine (Dexdomitor, Orion Corporation) and 70 mg/kg ketamine administered i.p. With the animal on its side, a microloader attached to a 10uL Hamilton syringe was inserted into one external naris such that it entered 7mm into the dorsal

recess. The animal was rotated onto its back and 2µL of 0.2% Triton was first injected to permeabilize cell membranes. After one minute, 2µL of dye (half of total) was injected. After 5 minutes the remaining 2µL was infused. After an additional 5 min the animal was rotated onto its side to allow the dye to reach all areas of the epithelium. The same procedure was performed on the contralateral side after an additional 15 min. Anesthesia was reversed with 1 mg/kg s.c. atipamezole (Antisedan, Orion Corporation). Mice were given 24-48 hours recovery time prior to further experimentation.

2.2.3 Pupillometry

Mice for pupillometry experiments were restraint trained and underwent cranial window implantation as above. Mice were head-fixed and positioned under a resonance-scanned (Neurolabware, Los Angeles, CA) titanium:sapphire ultrafast pulsed laser (Coherent Chameleon Ultra II) tuned to 920 nm (infrared). Images of the pupil were captured at 15.5 frames per second using a GigE camera sensitive to infrared light. IR light passed through the brain, transmitted through the orbit, and was emitted from the pupil. Pupil area was measured in each frame using custom software in Matlab based on the size of the circle that best fit the infrared light escaping the pupil. To mimic the illumination light during wide-field imaging, each pupillometry trial included illuminating the mouse with fiber optic-coupled blue light from a 470 nm LED identical to that used in the wide-field imaging apparatus (Thor Labs, Newton, NJ). Auditory stimuli were matched for position and sound pressure level. Two mice were excluded because the pupil was frequently obscured by partial closure of the lower eyelid, but exhibited qualitatively similar behavior to those reported here. An additional mouse was excluded because its pupil was completely dilated and exhibited no pupillary responses to

any stimulus, suggesting a ceiling effect. To improve signal-to-noise ratio, the average of the final three tone-present trials was calculated as a baseline for each mouse. Data were normalized for averaging across mice.

2.2.4 Olfactometry

Odorants were presented by a custom built eight-channel, air dilution olfactometer controlled by a computer running software written for MatLab (Mathworks). Nitrogen was passed through vials of pure odorant to produce a saturated carrier vapor that was then diluted into ~500 mL/minute ultrazero-humidity compressed air by computer-controlled mass flow controllers at a user-specified ratio. Wetted parts downstream of the odorants were made of PTFE or PEEK, and source gases were filtered by a hydrocarbon/moisture gas purification system (Chromatography Research Services). Stimulus onset and offset were controlled by a computer controlled valve that shunted a vacuum from and to an odorant-removal tube concentric with the odorant delivery tube after the manner of Kauer and Moulton (1974). The odorant delivery tube was placed within 2cm of the mouseôs nose. The odorants methyl valerate or butyl acetate (Sigma Aldrich, St. Louis, MO) were presented for 6-sec at a concentration of ~2% saturated vapor via vapor-dilution olfactometer using nitrogen as the carrier.

2.3 Surgical Procedures

2.3.1 Viral vector instillation

Mice were anesthetized with 1000 µg/kg dexmedetomadine (Dexdomitor, Orion Corporation) and 70 mg/kg ketamine administered i.p. with bupivicaine (~0.25 mL at 0.25%, s.c.) as a local anesthetic at the incision site. The scalp was shaved, washed with three cycles of Betadine and 70% ethanol and then surgically opened with a midline

incision. The periosteal membrane was removed and the skull dried with a 70% ethanol solution. An FG 1/2 burr was used to make a hole in the skull over each olfactory bulb. A gastight 1.0µL Hamilton syringe (1700 series; Hamilton Company) was used to infuse (Quintessential Stereotaxic Injector, Stolting) 0.5µL of AAV1.Syn.Flex.GCaMP6f.WPRE.SV40 (University of Pennyslvania Vector Core) into the glomerular layer at a rate of 0.1µL/minute. After infusion completion, the syringe remained in the tissue for five additional minutes to allow for diffusion. The process was then repeated for the contralateral olfactory bulb. The midline incision was closed and secured with either tissue adhesive (Vetbond, 3M) or interrupted 6.0 silicone coated braided sutures (Sofsilk, Covidien).

2.3.2 Headcap and cranial window implantation

Headcaps and cranial windows were implanted as previously reported (Czarnecki et al., 2012; Kass et al., 2013). Briefly, mice were anesthetized and surgically prepped as described in section 2.3.1. Following removal of the periosteal membrane, a custom acrylic headcap was secured using cyanoacrylate and dental acrylic and the skull overlying both olfactory bulbs was thinned to transparency using a dental drill with FG 2 burr and coated with a thin layer of cyanoacrylate. The wound margins were secured with tissue adhesive (Vetbond, 3M) and the window covered by a protective metal shield secured to the headcap. All animals were singly housed following headcap implantation.

2.3.3 Intranasal cannula surgery

An intranasal cannula was surgically implanted in the manner of Wesson et al. (2008). During cranial window surgery, the scalp over the frontonasal bone also retracted. The bone was cleaned with ethanol and a 0.7mm diameter hole was drilled

unilaterally approximately (visually guided to avoid visible capillaries) 3mm anterior to the frontal/nasal fissure and approximately centered on the medial/lateral axis. A custom made low profile pedestal with a 23g cannula was inserted into the dorsal recess and cemented in place. During the imaging session, a thermocouple (EMTSS-010 g-12; Omega) was inserted into the cannula in order to measure temperature change of intranasal airflow corresponding with respiratory inhalation and exhalation. Traces in Fig. 3 filtered with 9.3 Hz LP Butterworth temporal filter.

2.3.4 Tracheotomy

Prior to surgery, a borosilicate glass capillary tube (1B120F-4; World Precision) was heated, bent into an S-shape, and pulled and PE-50 tubing (Scientific Commodities, Inc) was pulled and secured onto the glass capillary tube in order to extend the opening of the capillary tube away from the thoracic cavity. Following cranial window implantation, mice were placed on their back and given bupivicane along the median cervical skin. This area was shaved and cleaned with alternating washes of 70% ethanol solution and Betadine surgical scrub. A single incision was made along this axis. The muscle was retracted to expose the trachea. An incision was made in the sublaryngeal region and the glass tube was inserted into the trachea with the open end facing the lungs and the other end outside the body. The tube was secured with suture that held the trachea tightly around the tube. The skin around the tracheal tube was then closed and secured with tissue adhesive (Vetbond, 3M). Animals were then secured to the head-holder and allowed to wake up in the widefield imaging apparatus. Mice breathed freely through the tracheal tube, with no airflow possible through the nasal passages. The tracheal tube was monitored for condensation and cleared when necessary.

2.4 Drug administration via intraperitoneal cannula

Mice were randomly assigned to receive either saline or CGP35348 infusions. Animals were lightly anesthetized with isoflurane (Aerrane, Baxter Healthcare, Deerfield, IL) and implanted with a pre-loaded length of polyethylene tubing (Intramedic PE 10, Becton Dickinson) via an 18G guide needle, attached to a 1.0mL syringe. CGP35348 or saline was administered via intraperitoneal cannula after 9 to 11 tone-present Expectation Induction trials were presented to collect a stable baseline. After drug infusion, Expectation Induction trials continued until OSN response amplitudes plateaued (range: 11 to 17 trials, with number of trials for control animals yoked to CGP-infused animals), at which point the tone-omitted Expectation Violation trial was administered.

2.5 Imaging methods

2.5.1 Widefield optical imaging of olfactory bulb function

For optical imaging, the protective shield overlying the cranial window was removed and the mouse was secured to the headholder. A drop of Ringerôs solution (140 mM NaCl, 5 mM KCl, 1mM $CaCl_2$, 1mM $MgCl_2$, 10mM HEPES and 10mM dextrose) and a glass coverslip was positioned over the cranial window to ensure a flat optical surface. Optical imaging was performed as previously described (Kass et al., 2013; Kass, Rosenthal et al., 2013). Briefly, the dorsal surface of both olfactory bulbs was visualized using a custom imaging apparatus including a 4x, 0.28 NA Olympus macro objective lens and images were acquired at 7 Hz (spH) or 25 Hz (Calcium Green or GCaMP) using a low-light, back-illuminated CCD camera with a resolution of 256x256 pixels (RedShirtImaging, Decatur, GA). Thermocouple signals were acquired at 100 Hz.

Epiillumination was provided by a 470-nm wavelength LED from ThorLabs (Newton, NJ).

2.5.2 Two-photon microscopy

Structural images were captured through a cranial window in anesthetized mice using a 2-photon microscope (Fig. 1C Neurolabware, Los Angeles, CA), 25x water immersion objective (Nikon, 1.1NA), with a resonance-scanning titanium:sapphire ultrafast pulsed laser (Coherent Chameleon Ultra II) with excitation wavelengths at 920-880 nm (GCaMP) and 800 (AlexaFlur 568-conjugated dextran amine). Data were acquired by open source Matlab software, Scanbox, at 15.62 Hz and 512 lines per frame.

2.6 Data analysis

2.6.1 Optical neurophysiology data analysis

Regions of interest corresponding to putative glomeruli were manually selected based on their odorant-evoked change in fluorescence. Responses to non-olfactory stimuli were not glomerular, but instead diffused throughout the olfactory bulb, so the entire dorsal olfactory bulb was used as a region of interest. For spH data, which produces an integrative signal, the response of each glomerulus was measured as the peak fluorescence within 4 sec of the odorant offset minus the pre-odor baseline fluorescence on each trial. For calcium data, inhalation-induced peaks in the fluorescence signal were measured relative to the pre-peak trough and normalized to the baseline fluorescence, producing a ΔF/F measure for each inhalation. Trials with obvious movement artifacts were discarded. Glomerular responses were pooled across mice where indicated. For non-olfactory and odor omission experiments, whole bulb ROIs were selected to capture diffuse non-glomerular signals.

2.6.2 Change Index Normalization

To facilitate comparisons across experiments, we expressed population averages in terms of a change index, defined as (test trial - reference trial)/(test trial + reference trial), after the manner of (Kato et al., 2012). This index equals -1 if the response on the test trial is completely abolished, equals 0 if the response on the test and reference trials are the same size, and asymptotically approaches 1 as the response on the test trials exceeds the reference trial. This approach is superior to traditional ñpercent changeò approaches because it prevents unidirectional bounding, i.e. that responses can be more than 100% increased but cannot be more than 100% decreased.

2.6.3 Quantification of Light Responses

PG cell populations responded to the onset of the microscope light at the beginning of each trial in awake animals. In most experiments, this response was completed by the onset of the tone or odorant 3 or 4 seconds later, allowing the response to those stimuli to be compared to the pre-stimulus baseline. However, the response to the light itself occurred almost immediately within each trial, requiring the comparison of the peak response relative to the post-response baseline.

PG cell populations exhibit a very stable resting oscillation on which stimulus-evoked responses ride. To separate light-evoked responses from this oscillation, the trial containing a light-evoked response was operationally defined as a trial in which the largest fluorescence peak in the first three seconds of the trial was at least double the size of the average last fluorescence peak within the first three seconds across trials.

2.6.4 Cumulative Frequency Display

Individual measurements displayed in cumulative frequency distributions (e.g. Fig. 5D) are expressed as raw values to show the relative distributions of response amplitudes on test and reference trials. These graphs permit the display of every data point from each experiment.

3. Results

3.1: Non-olfactory responses in the olfactory bulb

In mice expressing the calcium indicator GCaMP3 from the *gad2* locus, it is possible to selectively visualize the activity of GABAergic periglomerular interneurons (Shao et al., 2009; Fig. 1C). Through a chronically implanted cranial window, population-level GCaMP3 signals were quantified in awake, head-fixed mice using wide-field fluorescence microscopy during the presentation of sensory stimuli. As expected (Wachowiak et al., 2013), odor presentation evoked strong calcium signals in odor-specific spatial foci that corresponded to individual glomeruli (Fig. 2A&B, Odor). Unexpectedly, the population of *Gad2*-PG cells also made stimulus-locked responses to the presentation of a visual stimulus (the bright 470 nm light emitted from the microscope during imaging; Fig. 2A, Light), a somatosensory stimulus (the deflection of the mouseôs whiskers; Fig. 2A, Whisker), and an auditory stimulus (a 1 kHz, 74 db tone; Fig. 2A, Tone). Unlike the odor-evoked activity, these cross-modal responses were not spatially localized to a specific subset of glomeruli. They were generally smaller than the odor-evoked responses (Fig. 2C; mixed linear model $F(3, 15) = 15.72$, $p < 0.001$), but exhibited similar peak response latencies hundreds of milliseconds after stimulus onset (Fig. 2D; mixed linear model $F(3, 15) = 0.4$, $p = 0.75$). When the same mice were imaged under ketamine- dexmedetomadine anesthesia, the response to olfactory stimulation was qualitatively similar to that in waking mice, but the responses to cross-

modal stimulation (light, tone, and whisker brush) were completely eliminated (Fig. 2B). This selective effect of anesthesia on non-olfactory neural responding is consistent with the idea that cross-modal information is relayed to the olfactory bulb via higher sensory regions. Importantly, these responses were also observed in *Gad2*-cre mice with GCaMP6f expressed via intrabulbar viral vector infusion (Fig 2E), demonstrating that they arise from neurons in the OB and not from terminals of afferents entering from other brain regions.

3.2: Cross-modal responses are not due to changes in intranasal airflow

When surprised, many species including humans and mice make a sudden sharp inhalation, which in rodents is sometimes accompanied by a bout of fast investigatory sniffing (Verhagen et al., 2007). Cross-modal stimuli could potentially evoke rapid changes in intranasal airflow, which could conceivably in turn activate intranasal mechanoreceptors (Menco & Jackson, 1997; Grosmaitre et al. 2007; although mechanosensory signaling in the bulb has not been observed). To test for this potential mechanism, an intranasal cannula was surgically implanted in the bone overlying the nasal passage. A thermocouple, which is sensitive to changes in air temperature, was inserted into the cannula during imaging to record intranasal respiration during light only presentations. A direct correlation between sniffing and GCaMP3 signal was not observed (Figure 3A). Similar to previous findings of single unit activity in the mitral cell layer (Macrides & Chorover, 1972; Motokizawa & Ogawa, 1997), a change in respiration was sometimes paired with a change in PG cell activity (Fig $3A_i$), although the pattern was not consistent in magnitude (Fig $3A_{ii}$), nor did a change in respiration always occur when there was a non-olfactory response (Fig$3A_{iii}$). To experimentally

confirm that non-olfactory stimuli could induce PG cell activity in the absence of intranasal airflow, responses to cross-modal stimuli were observed in two acutely tracheotomized mice. Odor responses were not observed (Figure 3B), indicating efficacy of the tracheotomy and absence of intranasal airflow. However, the cross-modal responses persisted following tracheotomy (Figure 3B) showing that it is not intranasal airflow, but rather a centrifugal input, that drives interneuron responses to non-olfactory stimuli.

3.3: Cross-modal responses interact with expectation

In an attempt to understand how non-olfactory responses interact with expectation, the time between light presentations was manipulated. Mice were presented with 4 blocks of 15 3-second light only trials, with decreasing interstimulus intervals (ISIs) between blocks. ISIs were 108-, 36-, 12-, and 4-sec. These times span short, predictable intervals (4-sec) as well as longer intervals that are presumably more difficult to estimate accurately (and therefore for the presence of a stimulus to be more surprising). Light onset again evoked inhibitory interneuron activity (Fig. 4A) as in the experiment in section 3.3. Whole bulb analyses of maximum light-evoked GCaMP3 calcium transients in *Gad2*-PG cells significantly reduced (Fig 4A&B) with shorter ISIs (repeated measures ANOVA, $F(3) = 9.934$, $p < 0.001$). No interaction between within block trial number and ISI was found ($F(42) = 0.852$, $p = 0.21$; data not shown). Most of the maximal responses occurred in the beginning (first second; Fig4C) of the trial ($\chi^2 = 163.46$, $p < 0.001$). Trials were subsequently scored as either containing a light-evoked response or not containing a response (see section *2.5.2* for scoring details). The likelihood of a light-evoked response was higher at *longer* ISIs (Fig4D). That is, the

shorter the ISI, the less likely it is for a trial to contain a response to light onset ($G^2 = 8.91$, $p = 0.03$). This suggests that in circumstances in which a non-olfactory stimulus is more surprising, the olfactory bulb is more likely to respond.

3.4: Surprise alters inhibitory interneuron activity

Since it is possible for non-olfactory stimuli to evoke activity in inhibitory OB interneurons, to test the hypothesis that the olfactory bulb is sensitive to surprise, operationalized as *violations of expectations*, naïve *Gad2*-GCaMP3 mice were headfixed and presented with a High Surprise paradigm consisting of 13 consecutive light-tone-odor trials. On the 14th trial, the light and odor were presented with the same sequence and timing but the *tone was omitted* (Fig. 5A). To confirm that mice detect the change in stimulus contingency from the omission of the ñwarning toneò cue, we tested this paradigm in wild-type control animals while observing the mouseôs pupil[1]. When the odor was presented without the expected tone cue, we observed a distinct dilation of the mouseôs pupil that began shortly after odor onset and was absent on the preceding three tone-present trials (Fig. 5B). When the experiment was repeated in *Gad2*-GCaMP3 mice, on the tone-omitted trial the presentation of the odor evoked a significantly larger response (Fig. 5C-E) during the first odor inhalation than on the preceding tone-present trial (Wilcoxon signed ranks test $Z = -8.56$, $p < 0.001$; paired samples t-test $t(136) = -11.33$, $p < 0.001$). Representative maps show that the *Gad*2-PG cell activity was elevated diffusely across the dorsal bulb (Fig. 5E$_i$ & Fig. 7A). This suggests that surprising odor presentation evokes a global modulation of olfactory input across glomeruli.

[1] Pupillometry performed by collaborator Cynthia Fast.

3.5 Surprise alters olfactory input to the brain

GABA released from *Gad2*-PG cells binds to $GABA_B$ receptors on the presynaptic terminals of OSNs, activating a G-protein that suppresses N-type calcium conductance and thus neurotransmitter release (Wachowiak et al., 2005). Therefore, it was hypothesized that the increased response of *Gad2*-PG cells on the first inhalation of an odor presented without the expected ñwarningò tone would suppress calcium influx in the OSN presynaptic terminals. To test this hypothesis, the High Surprise paradigm was repeated in wild-type mice whose OSN presynaptic terminals were selectively labeled with the calcium-sensitive dye Calcium Green dextran via intranasal instillation and anterograde transport. These data indeed revealed a significant decrease in odor-evoked calcium flux in OSN terminals on the surprising tone-omitted trial (Fig. 6A-D; Wilcoxon signed ranks test $Z = -3.86$; $p < 0.001$; paired samples t-test $t(21) = 4.29$; $p < 0.001$). Importantly, this suppression was observed during the very first inhalation of odorant (Fig. 6B), reflecting a very rapid modulation of olfactory input.

Presynaptic calcium flux exhibits a non-linear and temporally complex relationship to neurotransmitter release, so we repeated the experiment a fourth time in mice where exocytosis from OSN axon terminal populations was visualized with the fluorescent exocytosis indicator synaptopHluorin (OSN-spH mice) (Bozza et al., 2004). Consistent with the presynaptic calcium data, repeating the tone-omission experiment in OSN-spH mice revealed a significant decrease in odor-evoked neurotransmitter release from OSN terminals on the surprising, tone-omitted trial (Fig. 6E-G) compared to the preceding tone-present trial (Wilcoxon signed ranks test $Z = -4.78$, $p < 0.001$; paired samples t-test $t(37) = 8.17$, $p < 0.001$).

Importantly, analysis of sniff-locked OSN calcium transients (Wachowiak & Cohen, 2001) revealed no difference in sniffing frequency (mixed-model ANOVA $F(1,40) = 0.41$, $p = 0.52$; Fig. 7) during the odor presentation on tone-omitted and tone-present trials in the High Surprise paradigm (Fig. 7B) despite the clear difference in OSN synaptic output during that time (Fig. 6A-B). Similarly, there is also no difference in sniff frequency under other conditions when the tone omission is not surprising ($F(1,40) = 2.08$, $p = 0.16$; Fig. 7 Low Surprise). The present results thus cannot be directly attributed to changes in odor sampling behavior (Verhagen et al., 2007). In mice (and unlike work in rats (Cenier et al., 2013), high-frequency investigatory sniffing is observed in some odor-guided behavioral tasks but not others and is more strongly predicted by reward availability than by odor presentation (Wesson et al., 2008).

To compare the spatial element of this expectation-based modulation across the dorsal olfactory bulb, we computed difference maps between the tone-cued and tone-omitted trials for the *Gad2*-GCaMP activity (Fig. 8A) OSN-spH signals (Fig. 8B), and OSN-Calcium Green signals (Fig.8C). Representative maps across neuron type and indicator show that signals were reduced in all of the glomerular foci activated by the test odor. Despite the altered odor-evoked response amplitudes, the relative patterns of odor-evoked OSN output across glomeruli (which represents odor identity) were highly correlated between the surprising and the tone-cued trials (Fig. 8D). This suggests that surprising odor presentation evokes a global modulation of olfactory input across glomeruli.

3.6: $GABA_B$ receptor activity is necessary for surprise-induced OSN suppression

To confirm that the information about tone-omission was being conveyed to OSNs via GABA release from OSNs, an extended version of the tone-omission experiment was performed in a group of OMP-spH mice in which the $GABA_B$ receptor antagonist CGP35348 (or vehicle control) was administered systemically midway through the baseline period. $GABA_B$ receptor blockade relieved the presynaptic inhibition of OSN terminals as expected, significantly enlarging the responses to the tone-cued odor compared to the pre-drug baseline (Fig. 9A&B; paired samples t-test $t(70) = -7.61$). As hypothesized, odor presentation on a tone-omitted test trial did not evoke any less neurotransmitter release ($t(67) = -1.33$; $p = 0.187$) from OSNs than odor presentation on the preceding tone-present trial in mice that received CGP35348 (Fig. 9A&C), consistent with the hypothesis that the reduced OSN synaptic output on tone-omitted trials is caused by $GABA_B$ receptor activation. Mice that received vehicle infusion showed no significant effect of infusion (Fig. 9D&E; paired samples t-test ($t(53) = -1.84$, $p = 0.19$) and did show the expected reduction ($t(53) = 7.67$; $p < 0.001$) in OSN output on the tone-omitted test trial (Fig. 9D&F). While it may seem counterintuitive for the olfactory system to suppress OSN neurotransmitter release when an odor is presented unexpectedly, in fact the suppression of glutamate release via presynaptic $GABA_B$ receptors can help prevent neurotransmitter depletion and AMPA receptor desensitization, thus increasing the synapsesô ability to sustain activity during periods of strong stimulation (McGann 2013; Murphy et al., 2004; Brenowitz & Trussell, 1998; Brenowitz & Trussell, 2001).

3.7 Tone omission must be surprising

The tone-omission design explicitly tests for a cognitive representation of the light-tone-odor sequence because the only way the *omission* of an auditory stimulus could affect olfactory processing is by violating the mouseôs expectation that odors are always preceded by tones. To further confirm this interpretation, we repeated the tone-omission experiment with an altered paradigm in which the tone had a 50% chance of omission during baseline trials and was omitted on the 14th trial as above (Fig 10A). In wild-type mice with Calcium Green-loaded OSNs, the odor-evoked response on the 14th trial (where the omission of the tone was not very surprising) was not significantly different ($t(19) = -0.9$, $p = 0.38$) than on the preceding tone-present trial (Fig. 10B-C). Notably, the odor responses were not different between tone-present and tone-omitted trials during the baseline trials ($t(20) = -1.01$, $p = 0.33$), demonstrating that the mere presence of a tone that does not strongly correlate with odor presentation had no effect on OSN output (Fig. 10C).

3.8 Animals must be awake

To confirm the importance of cross-modal input and rule out peripheral mechanisms, the High Surprise tone-omission experiments were repeated in anesthetized OMP-spH mice. No effect of tone omission was observed (Fig. 10E-G; Wilcoxon signed ranks test $Z = -0.13$, $p = 0.9$; paired samples t-test $t(59) = 1.72$, $p = 0.09$), consistent with the finding that cross-modal information does not reach the PG-OSN circuit in anesthetized mice.

3.9 Olfactory bulb inhibitory interneurons are sensitive to unexpected odor omissions

To test the hypothesis that cross-modal stimuli convey information about odor expectations to the olfactory bulb, naïve head-fixed *Gad2*-GCaMP3 mice were presented

with the High Surprise paradigm, with the induction phase again consisting of 13 consecutive light-tone-odor trials (Fig. 11A) at approximately one minute intervals. In this paradigm, the light and tone were both predictive of subsequent odor delivery. On the 14th trial (the test trial) the light and tone were presented with same timing as on the preceding trials but the *odor was omitted* (Fig. 11A). This allowed observation of the response evoked by the light and tone-cued expectation of an odor without presenting the odor itself. Remarkably, whole bulb analyses show that the peak response amplitude of the *Gad2*-PG cells during the period the odor was expected on the odor-omitted test trial was not significantly different than on the preceding light-tone-odor trial, even though no olfactory stimulus was actually presented (Fig. 11B & E; mixed model ANOVA $F(1,10) = 9.3$, $p < 0.05$, $\eta_p^2 = 0.48$). However, the response pattern was diffuse and did not resemble the focal pattern evoked by actual odor presentation (Fig. 11B). In a control group, the same paradigm was used but without any odors ever being presented (Fig. 11C). In these mice, endogenous *Gad2*-PG cell responses to the light and tone combination were observed (as in Fig. 2C), but they were significantly smaller than the responses to the same light and tone stimuli when they predicted an odor (Fig. 11D & E).

3.10 Surprise alters simultaneous multimodal odor expectations

In order to investigate the role of different auditory cues establishing the expectation of a specific odor, a modified High Surprise paradigm with two different tone frequencies and two similar odors in *Gad2*-GCaMP3 mice was performed. Tone A (1 kHz) was randomly paired with either the odor methyl valerate (MV) or the odor butyl acetate (BA) and tone B (5kHz) was paired with the other odor. After 13 interleaved pairings of each trial type, the odors were switched such that the tone now precedes the

alternative odor, with first incongruent odor counterbalanced between animals. Half of the animals experienced BA as the first tone-incongruent odor, while the other half received MV. The pattern of results was not different depending on which was the first incongruent odor (data not shown). Prior to the switch, the last tone-odor congruent trial of MV (9.22% qpF/F) induced a larger response amplitude (Fig. $12A_i$ left & D) on the first sniff after odor onset than that induced by BA (6.09% qpF/F; independent samples t-test $t(671) = -10.08$, $p < 0.001$; Fig. $12A_{ii}$ left & D). This illustrates innate difference in the ñnormalò neural response magnitude to these odorants. However, on the first tone-odor incongruent trial,when the mouse was expecting one odor but actually received the other odor, we observed a notable change in response magnitudes, but in different directions for MV and BA (Fig. $12A_i$&A_{ii}). The response to MV decreased from a change index of 0 when it was expected to -0.09 (Fig. 12C right) when the animal was putatively expecting BA, but actually received MV (paired samples t-test $t(382) = 7.19$, $p < 0.001$). Conversely, the response to BA increased (Fig. 12C left) from 0 to 0.12 when the mouse was expecting MV but actually received MV (paired samples t-test $t(289) = -6.73$, $p < 0.001$). These opposing effect directions make the amplitude of the neural responses to each odor more similar to each other.

Methyl valerate and butyl acetate have a qualitatively different spatial activation pattern on the dorsal olfactory bulbs, and continued to exhibit their distinctive spatial patterns even when a different odor was expected. How then could they exhibit different changes in their evoked response amplitudes? These results may be possible if the BA-associated tone cue induces preparation for a relatively small response and the MV-associated cue potentiates a larger response. PG cells are uniquely positioned, as they are

driven both by odor input via OSNs and other juxtaglomerular cells, which receive the bulk of top-down inputs. Therefore, the unexpected directionality of this experiment may reveal a complex system of potentiating and suppressing bottom-up inputs. The fact that the potentiation or suppression influences different glomeruli than the ones normally activated by the expected odor is consistent with the finding that cross-modal signals seem to be diffusely distributed over the OB (Fig. 2).

The use of two tones and two odors also makes it possible to reveal more information about the nature of the tone-evoked signals. Different frequency tones did not endogenously evoke a different amplitude response (Fig. 12E), as revealed by whole bulb analysis of the last congruent trial in all animals (independent samples t-test $t(11) = 0.694$, $p = 0.5$). Collapsing across odor type, the first incongruent trial did not evoke a different amplitude tone response than the previous, congruent trial (Fig. 12F; paired samples t-test $t(12) = -0.55$, $p = 0.59$). This is not surprising, since there is nothing yet incongruent about the trial (nothing was manipulated between the light onset and tone onset, the incongruence comes later with odor presentation). However, the second incongruent trial, occurring after animals may have the knowledge that incongruence is a possibility, also did not statistically alter tone-evoked response amplitude (Fig. 12F; paired samples t-test $t(12) = 0.999$, $p = 0.34$). This indicates first that non-olfactory PG-cell responses seemingly do not carry information about stimulus features *per se* and second that surprise in the olfactory domain does not necessarily induce subsequent changes in the response to the predictive cue.

4. Discussion

Most models of sensory processing presume that brain regions tasked with early sensory processing are limited to extracting the sensory inputs to their single sensory modality and presenting that ñbottom-upò information to higher brain regions for interpretation and contextualization. However, the present data indicate that in awake animals, simple cross-modal sensory information can be available as early as the initial sensory input to the brain ï even some of the first brain neurons to receive afferent olfactory signals from the periphery are also responsive to auditory, somatosensory, and visual stimuli. Early multisensory integration may thus play a more fundamental role than previously imagined, perhaps even in other sensory systems. It remains to be determined what underlying anatomical projections convey this information, what level of detail is communicated, and whether attentional mechanisms (Li & Cleland, 2013) or orienting behaviors (e.g. sniffing; Fukunaga et al., 2012; Verhagen et al., 2007; Shoenfeld & Cleland, 2006) play a role in this integration as well.

These neurophysiological data demonstrate that violating expectations about an upcoming odor induced rapid local modulation of the output of the olfactory nerve when expectations are violated. The effect of expectation on OSNs is particularly remarkable because they are the very first neurons in the entire olfactory system, transducing the odor into a neural signal at their dendrites in the olfactory epithelium and conveying that information to the central nervous system at their axon terminals in the olfactory bulb. These effects may occur either through neuromodulatory mechanisms or more focal cortically driven inputs into the olfactory bulb (Fig $1B_i$). In fact, neuromodulators are often implicated in surprise signals and attention (eg Preuschoff, Hart & Einhäuser, 2011; Yu & Dayan, 2005; Fellous & Linster, 1998).

Potential mechanisms: Neuromodulatory inputs

Wheat germ agglutinin-horseradish peroxidase (WGA-HRP) injections in the glomerular layer of the OB revealed labeled neurons in the dorsal and median raphé (McLean & Shipley, 1987). Autoradiographic analysis of tritiated ([^{3}H]) serotonin (5-HT) showed similar connections from the OB mostly to the ipsilateral dorsal raphé after injecting [^{3}H]-5-HT into the granule cell layer, with some accumulation in the glomerular and plexiform layers (Araneda et al., 1980). Deafferenting serotonergic fibers in the OB by injecting 5,7-dihydroxytryptamine into the descending pathway induced atrophy in the glomerular, granular cell, internal, and external plexiform layers. After bulbar serotonergic deafferentation, there was a reduction in glomerular synaptic density, loss of afferent terminals, but no observed changes in mitral and tufted cell dendrites (Moriizumi et al., 1994). Functionally, stimulating the raphé increases both tonic and odor-evoked responses of both PG and SA interneurons, putatively through ET cells (Brunert et al., 2016). WGA-HRP tracing studies show heavy, primarily ipsilateral, noradrenergic connections from LC to the OB (Shipley et al., 1985). In the rat, it was estimated that 38% of LC neurons synapse in the OB (Shipley et al., 1985). LC neurons appeared in the granule cell layer as well as the glomerular layer, where it appears that one LC neuron enters a single glomerulus (Shipley et al., 1985). Similar WGA-HRP tracing experiments reveal cholinergic fibers in the granule cell and glomerular layers of the OB originating from the horizontal limb of the diagonal band of Broca (HDB) (Heimer et al., 1990) and autoradiography reveals muscarinic receptors in the glomerular, mitral, and granule cell layers with particularly high density in the external plexiform layer (Rotter et al., 1979).

Potential mechanisms: Cortical inputs

In addition to neuromodulatory areas, cortical areas also send feedback connections to various layers of the OB. This may be important in such paradigms as experiment in 3.3 in that using two different cues and two different odors may induce more specific expectations and/or memories. This would hypothetically engage more cortico-bulbar top-down inputs than neuromodulatory inputs.

Innervation from olfactory cortex principle cells synapse mostly onto granule cells and are likely restricted to glomerular columns, unlike the broader neuromodulatory input (Restrepo et al., 2009 for review). Electrolytic lesion including the prepiriform cortex, olfactory tubercle, and lateral olfactory tract results in degeneration in the OB, including the glomerular layer (Heimer, 1968). Injecting channelrhodopsin-2 (ChR2) into the anterior piriform cortex (APC) results in labeled cells in the ipsilateral granule and glomerular layers with minor labeling in the mitral and plexiform cell layers (Boyd et al., 2012). Similarly, photostimulating ChR2-infected PCx pyramidal cells reveals modulation of periglomerular and granule cells. When cortical photostimulation occurs during an odor presentation, the net result is a reduction of odor-evoked mitral cells activity, even though resting M/T activity was not altered (Boyd et al., 2012). ChR2-EYFP labeling shows AON axons reach the granule, external plexiform and glomerular cell layers, mostly with ipsilateral contacts (Boyd et al., 2012; Rothermel & Wachowiak, 2014). Photostimulation in the AON reveals a mixed response in MT cells (net inhibitory current), with excitation most likely monosynaptic directly from AON and inhibition disynaptic through the glomerular layer (Markopoulos et al., 2012). In the glomerular layer, PG and SA cells were both excited after AON photostimulation. Calcium imaging in bulbar AON axon terminals reveals modulation even in the absence of an odor and

during HDB electrical stimulation (Rothermel & Wachowiak, 2014). Taken together, it is clear that there are numerous ways in which cortical and subcortical areas can modulate several cell types in the OB to functionally alter early olfactory processing, potentially as early as in the primary sensory neurons.

Although physiological evidence is mounting suggesting the powerful role of top-down input to the olfactory bulb, the functional role of these inputs is still unknown. A recent study showed olfactory cortex derived sharp waves during slow wave sleep induced sharp waves in the olfactory bulb (Manabe et al., 2011). This synchronous activity potentiates the synapses onto adult born granule cells in the OB. Stimulating centrifugal axons induces granule cell apoptotic elimination (Komano-Inoue et al., 2014). This may support circuit reorganization after learning. Postprandial behaviors also show similar sharp waves, perhaps functioning akin to hippocampal replay (Komano-Inoue et al., 2014).

Implications

These experiments show that ñdedicatedò sensory areas are be more multimodal than previously believed. Non-olfactory stimuli are capable of driving responses in neurons that synapse onto primary sensory afferents. This activity driven solely by other modalities could have the capacity to directly shape primary odor representation. By manipulating the timing of non-olfactory stimulus presentations, it appears that only non-olfactory stimuli, which are surprising or relevant to an impending odor, are gated into the olfactory bulb. Non-olfactory responses persisting after tracheotomy suggests a central origination of these signals. Indeed, higher order cognition based on multimodal expectations was also shown to alter odor primary representations. The olfactory bulb is

privy to a sophisticated set of expectations regarding the entire sensory environment, at least under the right circumstances.

With such a wide range of neuroanatomical possibilities to instantiate expectations and ñhigher order cognitionò into the olfactory bulb microcircuit, it may be the case that they are engaged under different conditions. Here, multiple paradigms were used to show top-down influences on two neural populations. This may speak to there being multiple top-down mechanisms, dependent upon the source of the expectation. Perhaps simpler (as in the tone and odor omission paradigms), short-term expectations are expressed through neuromodulatory areas whereas more specific (as in the tone-odor switch paradigm) or long-term learning about expectations would be expressed via the more precise cortical inputs. Different top-down mechanisms may also induce different consequences for the olfactory coding and eventually, percept. While in these experiments, no changes in odor-driven spatial activity was observed, it may be the case that this occurs under different conditions. It is also important to keep in mind that animals in these experiments were not engaged in a task. Should task demands necessitate disambiguating a mixture, for example, there may be additional effects to the changes in amplitudes seen here.

There are many possibilities at to what these non-olfactory signals represent. Inhibitory interneuron activity may be a sniffing efferent copy. Although no evidence of the bulb receiving explicit information about sniffing exists, it has been postulated that the bulb may receive such an input since it is only two synapses away from subcortical respiratory areas (Ravel, Caille & Pager, 1987). The medial parabrachial nucleus sends projections to the preoptic magnocellular nucleus which then projects to the olfactory

bulb (Ravel, Caille & Pager, 1987). It is also worth noting that while some neural populations in the OB change activity following tracheotomy (Ravel & Pager, 1990) that was not the case in the PG cells imaged here. This indicates that these interneurons are not coupled to respiratory-driven oscillations. PG cell activity may also reflect an attentional signal, as they were modulated by timing-based expectations, and changes are only observed when cue omissions are surprising.

Indeed, by presenting visual and auditory cues at regular intervals preceding odor delivery and then omitting either a predictive cue or the odor itself reveals different activity in OSNs and PG interneurons. Many attention- or surprise-based changes in sensory processing rely on averages of many trials to see differences (e.g. auditory oddball). Here, these effects are robust enough to be seen in single trial comparisons. So robust in some cases, that the omission of an odor elicits the same magnitude of inhibitory interneuron activity as that driven by an odor itself (albeit in different populations of neurons). Tones at shorter intervals, or unsurprising odor absence, are not capable of driving this magnitude of response. This shows there is an interaction between olfactory system relevance and non-olfactory responses and suggests attentional mechanisms may be involved in these findings.

Despite the novelty of the current findings, conceptually related effects following violations of expectations have been documented in other brain areas. For instance, ñerrorò or ñteachingò signals have been well documented in the ventral tegmental area and substantia nigra (Schultz, Dayan & Montague, 1997; Stuber et al., 2008; Tobler, Dickinson, & Schultz, 2003) when a reward following a conditioned cue is not delivered as anticipated. When the reward is delayed (Apicella et al., 1992) or cues vary in

probability of reward (Fiorillo, Tobler & Schultz, 2003), neurons change temporal and magnitude of response. It is postulated that these responses to violations of expectation could inform new associations. Surprise and attention have long been an important concept in learning associations between stimuli, but here, it was shown that these cognitive effects could reach all the way to the input into the brain.

Furthermore, efficient anticipatory coding has been proposed in areas such as the retina (Hosoya, Baccus & Meister, 2005), though this makes use of low level mechanisms such as adaptation rather than utilizing top-down connections as found here. While it is true that adaptation creates a filter such that a sensory organ may be more sensitive to novel stimuli, this is theoretically very different from using descending projections to instantiate a sensory expectation derived from cognition (presumably even expectations the organism may be explicitly aware of). Work on unsupervised learning in perception postulates that higher cortical areas extract and calculate stimulus features of increasing complexity (e.g. Fiser & Aslin, 2001). If this is the case and cortical areas project back down to pre-cortical sensory regions, then it may be advantageous to conceptualize sensory inputs themselves as potentially being modified by expectations. Or, as in Bayesean learning, there may be a neural comparison between expectations (or priors) versus sensory stimulation. The precise consequences of these putative computations on perception and subsequent learning remain to be elucidated.

Ultimately, since it was shown that early primary sensory areas are privy to non-modality specific information, then subsequent areas may also contain more highly processed information than previously believed. Indeed, here it was shown that violations of expectations have the capacity of changing the very *input* into the brain.

Although it remains to be seen whether the output of the olfactory bulb is also different, PG cell signaling could be driven by and can drive activity in other olfactory bulb neural populations. An expectation *in and of itself* driving activity early in a primary sensory area also indicates how potentially strong these top-down inputs are to shape primary sensory representations. In fact, the modulation of interneurons by non-olfactory stimuli and primary sensory activity by cognitive factors suggests that there may be no such thing as a purely bottom-up sensory representation in the olfactory system.

References

Abraham, N.M, Spors, H, Carleton, A., Margrie, T.W., Kuner, T. & Schaefer, A.T. Maintainign accuracy at the expense of speed: Stimulus similarity defines odor discrimination time in mice. *Neuron* **44**: 865-876.

Apicella, P., Scarnati, E., Ljungberg, T. & Schultz, W. Neuronal activity in monkey striatum related to the expectation of predictable environmental events. *Journal of neurophysiology* **68**: 945-60.

Aro, M., Suzuki, M., Katayama, J. & Yagi, A. An odorant congruent with a color cue is selectively perceived in an odour mixture. *Perception* **41**: 474-82 (2012).

Aungst, J.L, Heyward, P.M., Puché, A.S., Karnup, S.V., Hayar, A., Szabo, G. & Shipley, M.T. Centre-surround inhibition among olfactory bulb glomeruli. *Nature* **426**: 623-629 (2003).

Bar, M. A cortical mechanism for triggering top-down facilitation in visual object recognition. *Journal of Cognitive Neuroscience* **15**: 600-9 (2003).

Bar, M. Visual objects in context. *Nature Reviews Neuroscience* **5**: 617-29 (2004).

Boyd AM, Sturgill JF, Poo C, Isaacson JS. Cortical feedback control of olfactory bulb circuits. *Neuron* **76**: 1161-74 (2012).

Bozza, T., McGann, J. P., Mombaerts, P. & Wachowiak, M. In vivo imaging of neuronal activity by targeted expression of a genetically encoded probe in the mouse. *Neuron* **42**, 9-21 (2004).

Brenowitz, S. & Trussell, L. O. Minimizing synaptic depression by control of release probability. *The Journal of neuroscience*, 1857-1867 (2001).

Brenowitz, S., David, J. & Trussell, L. Enhancement of synaptic efficacy by presynaptic GABA(B) receptors. *Neuron* **20**, 135-141 (1998).

Brunert, D., Tsuno, Y., Rothermel, M., Shipley, M.T. & Wachowiak, M. Cell-type-specific modulation of sensory responses in olfactory bulb circuits by serotonergic projections from the raphe nuclei. *The Journal of neuroscience* **36** 6820-6835 (2016).

Buck, L.B. Olfactory receptors and odor coding in mammals. *Nutrition Reviews* **62**: S184-8 (2004).

Buck, L.B. & Axel, R. A novel multigene family may encode odorant receptors: A molecular basis for odor recognition. *Cell* **65**, 175-187.

Cajal, SR. *Histologie du système Nerveux de l'Homme et des Vertebres*, Vol. II. Paris: Maloine (1911).

Czarnecki, L. A. *et al.* In vivo visualization of olfactory pathophysiology induced by intranasal cadmium instillation in mice. *Neurotoxicology* **32**, 441-449, doi:10.1016/j.neuro.2011.03.007 (2011).

Czarnecki, L. A. *et al.* Functional rehabilitation of cadmium-induced neurotoxicity despite persistent peripheral pathophysiology in the olfactory system. *Toxicological sciences : an official journal of the Society of Toxicology* **126**, 534-544, doi:10.1093/toxsci/kfs030 (2012).

Dalton P. Odor perception and beliefs about risk. Chemical senses 21: 447-58 (1996).

de Araujo, I. E., Rolls, E. T., Velazco, M. I., Margot, C. & Cayeux, I. Cognitive modulation of olfactory processing. *Neuron* **46**, 671-679 (2005).

de Olmos, J., Hardy, H. & Heimer, L. The afferent connections of the main and the accessory olfactory bulb formations in the rat: An experimental HRP-study. *Journal of Comparative Neurology* **181**, 213-244 (1978).

Devore, S. & Linster, C. Noradrenergic and cholinergic modulation of olfactory bulb sensory processing. *Frontiers in behavioral neuroscience* **6** (2012).

Distel H, Hudson R. Judgment of odor intensity is influenced by subjects' knowledge of the odor source. *Chemical senses* **26**: 247-51 (2001).

Elder, R.S., & Krishna, A., The effects of advertising copy on sensory thoughts and perceived taste. *Journal of Consumer Research* **36**: 748-756.

Fellous, J-M. & Linster, C. Computational models of neuromodulation. *Neural computation* **10**: 771-805 (1998).

Fiorillo, C.D., Tobler, P.N., Schultz, W. Discrete coding of reward probability and uncertainty by dopamine neurons. *Science* **299**, 1898-1902.

Fiser, J. & Aslin, R.N. Unsupervised statistical learning of higher-order spatial structures from visual scenes. *Psychological Science* **12**: 499-504 (2001).

Fukunaga, I., Berning, M., Kollo, M., Schmaltz, A. & Schaefer, A. T. Two distinct channels of olfactory bulb output. *Neuron* **75**, 320-329, doi:10.1016/j.neuron.2012.05.017 (2012).

Golgi C. Sulla fina struttura dei bulbi olfactorii. Rivista Sperimentale di Freniatria e Medicina Legale **1**: 405-25 (1875).

Gottfried, J. A. & Dolan, R. J. The nose smells what the eye sees: crossmodal visual facilitation of human olfactory perception. *Neuron* **39**, 375-386 (2003).

Grosmaitre, X., Santarelli, L.C., Tan, J., Luo, M & Ma, M. Dual functions of mammalian olfactory sensory neurons as odor detectors and mechanical sensors. *Nature neuroscience* **10**: 348-54 (2007).

Haberly, L.B. & Prince, J.L. The axonal projection patterns of the mitral and tufted cells of the olfactory bulb in the rat. *Brain Research* **129**: 152-157 (1977).

Hamilton, K.A., Heinbockel, T., Ennis, M., Szabó, G., Erdélyi, F., Hayar, A. Properties of external plexiform layer interneurons in mouse olfactory bulb slices. *Neuroscience* **133**: 819-829 (2005).

Heimer, L, Zahm, D.S., Schmued, L.C. The basal forebrain projection to the region of the nuclei gemini in the rat: A combined light and electron microscopic study employing horseradish peroxidase, fluorescent racers and *Phaseolus vulgaris*-leucoagglutinin. *Neuroscience* **34**: 707-731 (1990).

Heimer L. Synaptic distribution of centripetal and centrifugal nerve fibres in the olfactory system of the rat. An experimental anatomical study. *Journal of anatomy* **103**: 413-32 (1968).

Henderson JM, Hollingworth A. High-level scene perception. *Annual review of psychology* **50**: 243-71 (1999).

Herz, R. S. & von Clef, J. The influence of verbal labeling on the perception of odors: evidence for olfactory illusions? *Perception-London* **30**, 381-392 (2001).

Hosoya, T., Baccus, S.A. & Meister, M. Dynamic predictive coding by the retina. *Nature*. **436:** 71-77 (2005).

Johnson, B.A. & Leon, M. Modular representations of odorants in the glomerular layer of the rat olfactory bulb and the effects of stimulus concentration. *Journal of comparative neurobiology* **422**: 496-509 (2000).

Kass, M. D., Rosenthal, M. C., Pottackal, J. & McGann, J. P. Fear learning enhances neural responses to threat-predictive sensory stimuli. *Science* **342**, 1389-1392, doi:10.1126/science.1244916 (2013).

Kato, H. K., Chu, M. W., Isaacson, J. S. & Komiyama, T. Dynamic sensory representations in the olfactory bulb: modulation by wakefulness and experience. *Neuron* **76**, 962-975, doi:10.1016/j.neuron.2012.09.037 (2012).

Keller, A., *et al*. Functional organization of rat olfactory bulb glomeruli revealed by optical imaging. *The journal of neuroscience* **18**: 2602-12 (1998).

Komano-Inoue, S., Manabe, H., Ota, M., Kusumoto-Yoshida, I., Yokoyama, T.K, Mori, K. & Yamaguchi, M. Top-down inputs from the olfactory cortex in the postprandial period promote elimination of granule cells in the olfactory bulb. *European journal of neuroscience* **40**: 2724-33 (2014).

Kosaka, T. & Kosaka, K. Tyrosine hydroxylase-positive GABAergic juxtaglomerular neurons are the main source of the interglomerular connections in the mouse main olfactory bulb. *Neuroscience research* **60**: 349-54 (2008).

Kosaka, K., *et al*. Chemically defined neuron groups and their subpopulations in the glomerular layer of the rat main olfactory bulb. *Neuroscience research* **23**: 73-88 (1995).

Koulakov, A., Gelperin, A. & Rinberg, D. Olfactory coding with all-or-nothing glomeruli. *Journal of neurophysiology* **98**: 3134-42.

Li, G. & Cleland, T. A. A two-layer biophysical model of cholinergic neuromodulation in olfactory bulb. *The Journal of neuroscience* **33**, 3037-3058, doi:10.1523/JNEUROSCI.2831-12.2013 (2013).

Liu, S., Puché, A.C. & Shipley, M.T. The interglomerular circuit potently inhibits olfactory bulb output neurons by both direct and indirect pathways. *The Journal of neuroscience* **36**: 9604-17 (2016).

Macrides, F. & Chorover, S.L. Olfactory bulb units: Activity correlated with Inhalation Cycles and Odor Quality. *Science* **175**: 84-87 (1972).

Malnic, B., Hirono, J., Sato, T. & Buck, L.B. Combinatorial receptor codes for odors. *Cell* **96**: 713-23.

Manabe, H., Kusumoto-Yoshida, I., Ota, M. & Mori, K. Olfactory cortex generates synchronized top-down inputs to the olfactory bulb during slow-wave sleep. *The Journal of Neuroscience* **22**: 8123-8133 (2011).

Markopoulos, F., Rokni, D., Gire, D. H. & Murthy, V. N. Functional properties of cortical feedback projections to the olfactory bulb. *Neuron* **76**, 1175-1188, doi:10.1016/j.neuron.2012.10.028 (2012).

Menco, B. Ph. M. & Jackson, J.E. Cells resembling hair cells in developing rat olfactory and nasal respiratory epithelia. *Tissue & cell* **29**: 293-306 (1997).

McLean, J. H. & Shipley, M. T. Serotonergic afferents to the rat olfactory bulb: I. Origins and laminar specificity of serotonergic inputs in the adult rat. *The Journal of neuroscience* **7**, 3016-3028 (1987).

McGann, J. P. Presynaptic inhibition of olfactory sensory neurons: new mechanisms and potential functions. *Chemical senses* **38**, 459-474, doi:10.1093/chemse/bjt018 (2013).

McGann, J. P. *et al.* Odorant representations are modulated by intra- but not interglomerular presynaptic inhibition of olfactory sensory neurons. *Neuron* **48**, 1039-1053, doi:10.1016/j.neuron.2005.10.031 (2005).

Mitchell, D. J., Kahn, B. E. & Knasko, S. C. There's something in the air: effects of congruent or incongruent ambient odor on consumer decision making. *Journal of Consumer Research*, 229-238 (1995).

Mombaerts, P., *et al*. Visualizing an olfactory sensory map. *Cell* **87**: 675-86.

Moriizumi, T., Tsukatani, T., Sakashita, H. & Miwa, T. Olfactory disturbance induced by deafferentation of serotonergic fibers in the olfactory bulb. *Neuroscience* **61**, 733-738 (1994).

Morrot G, Brochet F, Dubourdieu D. The color of odors. *Brain and language* **79**: 309-20 (2001).

Motokizawa, F. & Ogawa, Y. Discharge properties of mitral/tufted cells in the olfactory bulb of cats. *Brain research* **763**: 285-7 (1997).

Murphy GJ, Glickfeld LL, Balsen Z, Isaacson JS. Sensory neuron signaling to the brain: properties of transmitter release from olfactory nerve terminals. The *Journal of neuroscience* **24**: 3023-30 (2004).

Petzold, G. C., Hagiwara, A. & Murthy, V. N. Serotonergic modulation of odor input to the mammalian olfactory bulb. *Nature neuroscience* **12**, 784-791, doi:10.1038/nn.2335 (2009).

Preuschoff, K., Hart, B.M. & Einhäuser, W. Pupil dilation signals surprise: evidence for noradrenalineôs role in decision making. *Frontiers in neuroscience* **5**, 115 (2011).

Price, J.L. & Powell, T.P. An experimental study of the origin and the course of the centrifugal fibres to the olfactory bulb in the rat. Journal of anatomy **107**: 215-37 (1970).

Ravel, N., Caille, D. & Pager, J. A centrifugal respiratory modulation of olfactory bulb unit activity: A study on acute rate preparation. *Experimental Brain Research* **65**: 623-628.

Ravel, N. & Pager, J. Respiratory patterning of the rat olfactory bulb unit activity: nasal versus tracheal breathing. *Neuroscience letters* **115**: 213-8 (1990).

Restrepo, D., Doucette, W., Whitesell, J. D., McTavish, T. S. & Salcedo, E. From the top down: flexible reading of a fragmented odor map. *Trends in neurosciences* **32**, 525-531 (2009).

Rothermel M, Wachowiak M. Functional imaging of cortical feedback projections to the olfactory bulb. *Frontiers in neural circuits* **8**: 73 (2014).

Rotter, A., Birdsall, N.J.M., Burgen, A.S.V., Field, P.M., Hulme, E.C., Raisman, G. Muscarinic receptors in the central nervous system of the rat. I. Technique for autoradiographic localization of the binding of [^{3}H]propylbenzilycholine mustard and its distribution in the forebrain. *Brain Research Reviews* **1**: 141-165 (1979).

Scalia, F. & Winans, S.S. The differential projections of the olfactory bulb and accessory olfactory bulb in mammals. *Journal of Comparative Neurology* **161**: 31-55 (1975).

Schoenfeld, T. A. & Cleland, T. A. Anatomical contributions to odorant sampling and representation in rodents: zoning in on sniffing behavior. *Chemical senses* **31**, 131-144, doi:10.1093/chemse/bjj015 (2006).

Schultz W., Dayan, P. & Montague, R. A Neural Substrate of Prediction and Reward. *Science* **275**: 1593-99 (1997).

Stuber GD, Klanker M, de Ridder B, Bowers MS, Joosten RN, et al. 2008. Reward-predictive cues enhance excitatory synaptic strength onto midbrain dopamine neurons. Science 321: 1690-2

Shao, Z., Puche, A.C., Kiyokage, E., Szabo, G. & Shipley, M. Two GABAergic intraglomerular circuits differentially regulate tonic and phasic presynpatic inhibition of olfactory nerve terminals. *Journal of Neurophysiology* **101**: 1988-2001 (2009).

Shipley, M. T. & Ennis, M. Functional organization of olfactory system. *Journal of neurobiology* **30**, 123-176 (1996).

Shepherd GM, Chen, W.R., and Greer, C.A. Olfactory Bulb in The Synaptic Organization of the Brain, ed. GM Shepherd, pp. 165-216. New York: Oxford University Press (2004).

Shulman, G. L. *et al.* Top-down modulation of early sensory cortex. *Cerebral Cortex* **7**, 193-206 (1997).

Sohoglu E, Peelle JE, Carlyon RP, Davis MH. Predictive top-down integration of prior knowledge during speech perception. *The Journal of neuroscience : the official journal of the Society for Neuroscience* **32**: 8443-53 (2012).

Spence, C., Levitan, C. A., Shankar, M. U. & Zampini, M. Does food color influence taste and flavor perception in humans? *Chemosensory Perception* **3**, 68-84 (2010).

Stevenson RJ. Associative Learning and Odor Quality Perception: How Sniffing an Odor Mixture Can Alter the Smell of Its Parts. *Learning and Motivation* **32**: 154-77 (2001).

Stuber, G.D, Klanker, M., de Ridder, B., Bowers, M.S., Joosten, R.N., Feenstra, M.G. & Bonci, A. Reward-predictive cues enhance excitatory synaptic strength onto midbrain dopamine neurons. *Science* **3321**: 1690-2 (2008).

Suzuki, Y., Kiyokage, E., Sohn, J., Hioki, H. & Toida, K. Structural basis for serotonergic regulation of neural circuits in the mouse olfactory bulb. *The Journal of comparative neurology* **523**, 262-280, doi:10.1002/cne.23680 (2015).

Taniguchi, H. *et al.* A resource of Cre driver lines for genetic targeting of GABAergic neurons in cerebral cortex. *Neuron* **71**, 995-1013, doi:10.1016/j.neuron.2011.07.026 (2011).

Tobler P.N., Dickinson A. & Schultz W. Coding of predicted reward omission by dopamine neurons in a conditioned inhibition paradigm. *The Journal of neuroscience* **23**: 10402-10 (2003).

Verhagen, J. V., Wesson, D. W., Netoff, T. I., White, J. A. & Wachowiak, M. Sniffing controls an adaptive filter of sensory input to the olfactory bulb. *Nature neuroscience* **10**, 631-639, doi:10.1038/nn1892 (2007).

Wachowiak, M. & Cohen, L. B. Representation of odorants by receptor neuron input to the mouse olfactory bulb. *Neuron* **32**, 723-735 (2001).

Wachowiak, M. *et al.* Inhibition of olfactory receptor neuron input to olfactory bulb glomeruli mediated by suppression of presynaptic calcium influx. *Journal of neurophysiology* **94**, 2700-2712, doi:10.1152/jn.00286.2005 (2005).

Wachowiak, M. *et al.* Optical dissection of odor information processing in vivo using GCaMPs expressed in specified cell types of the olfactory bulb. *The Journal of neuroscience : the official journal of the Society for Neuroscience* **33**, 5285-5300, doi:10.1523/JNEUROSCI.4824-12.2013 (2013).

Wesson, D.W., Donahou, T.N., Johnson, M.O. & Wachowiak, M. Sniffing behavior of mice during performance in odor-guided tasks. *Chemical senses* **33**, 581-596 (2008).

Yu, A.J. & Dayan, P. Uncertainty, neuromodulation, and attention. *Neuron* **46**, 681-692.

Zariwala, H. A. *et al.* A Cre-dependent GCaMP3 reporter mouse for neuronal imaging in vivo. *The Journal of neuroscience : the official journal of the Society for Neuroscience* **32**, 3131-3141, doi:10.1523/JNEUROSCI.4469-11.2012 (2012).

Zelano, C., Mohanty, A. & Gottfried, J. A. Olfactory predictive codes and stimulus templates in piriform cortex. *Neuron* **72**, 178-187, doi:10.1016/j.neuron.2011.08.010 (2011).

Zellner, D. A. & Kautz, M. A. Color affects perceived odor intensity. *Journal of Experimental Psychology: Human Perception and Performance* **16**, 391 (1990).

Zellner, D. A. & Whitten, L. A. The effect of color intensity and appropriateness on color-induced odor enhancement. *The American journal of psychology* (1999).

Zou, D-J., Chesler, A. & Firestein, S. How the olfactory bulb got its glomeruli: A just so story? *Nature reviews neuroscience* **10**: 611-618 (2009).

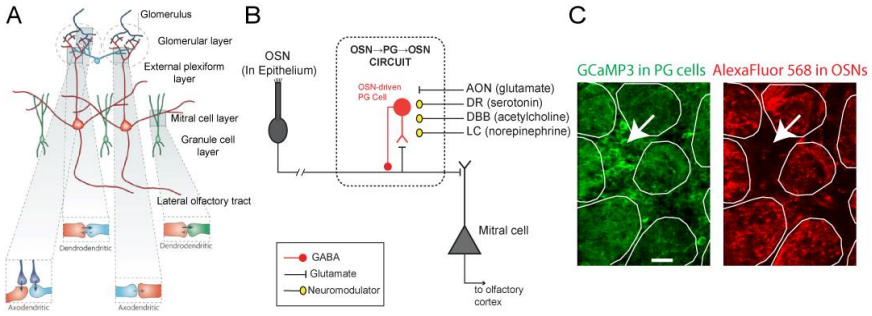

Figure 1. The olfactory bulb has circuitry consisting of top-down and bottom-up inputs. *A.)* Modified from Zou et al., (2009). OSNs (dark blue) enter the olfactory bulb and form glomeruli with dendrites of M/T cells (red) and subpopulations of juxtaglomerular cells (light blue). Granule cells (green) extend apical dendrites to the external plexiform layer. M/T cells extend axons out of the OB forming the lateral olfactory tract. *B)* Schematic of OB circuitry showing convergence of OSN input with projections from higher brain areas in the OSN-periglomerular cell (PG) circuit. *B)* 2-photon image of OSNs (red) anterogradely labeled from the nasal epithelium with surrounding Gad65-expressing PG interneurons (green).

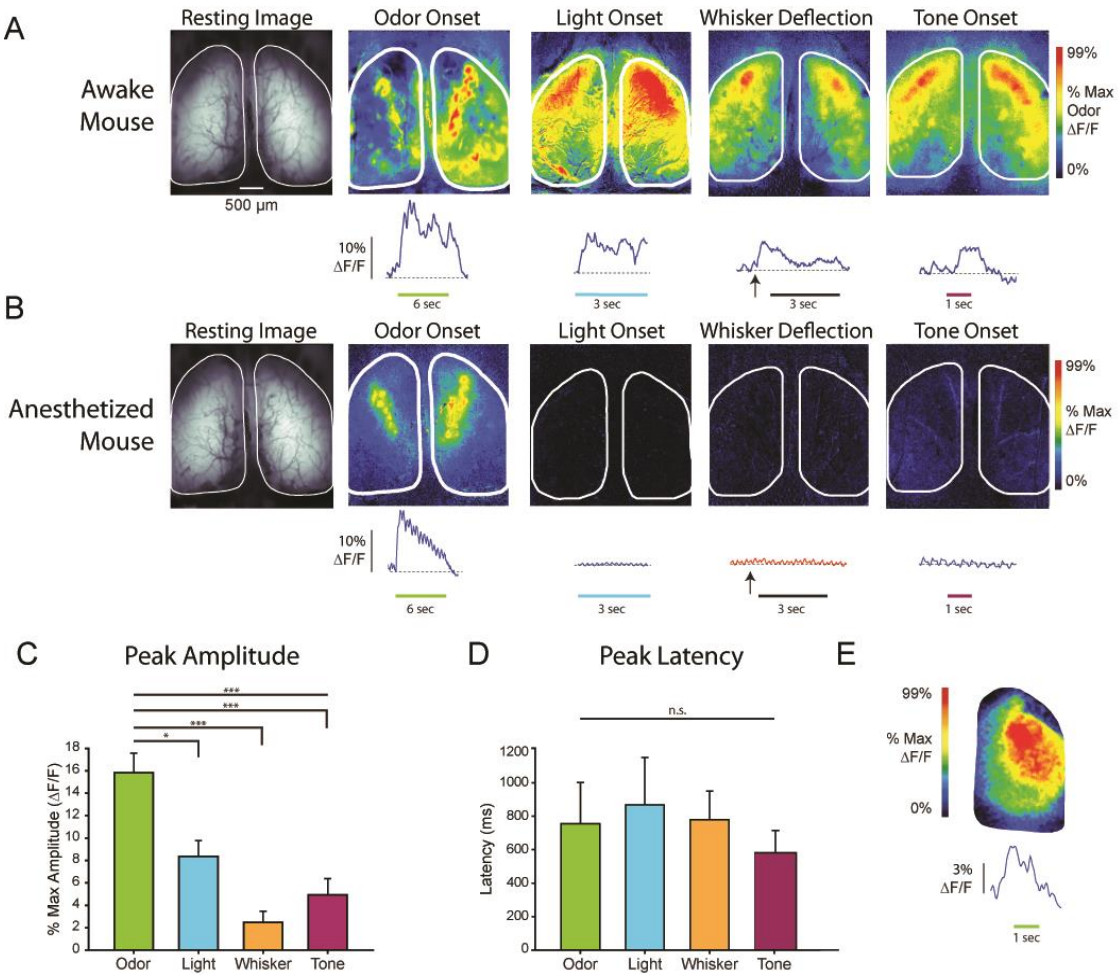

Figure 2. Olfactory bulb periglomerular interneurons receive cross-modal sensory input. *A)* Representative pseudocolor maps, scaled to odor maximum (top) and individual maxima (bottom), and fluorescence traces showing stimulus-evoked calcium signals in GAD65-PG cells in awake mice. Colored bar or arrow notes stimulus presentation and duration. *B)* Only olfactory responses were observed while under anesthesia (same animals as in A). *C)* Whole-bulb analyses revealed modality-dependent GCaMP3 peak amplitudes in awake mice (7 mice; mean ± SEM) with odorants evoking significantly larger responses than all other modalities (Tukeyôs HSD). *** p Ò 0.001 * $p < 0.05$ *D)* with no difference in latency to peak response. *E)* Pseudocolor response map to light-evoked response expressing GCaMP6f AAV via local olfactory bulb injection in inhibitory interneurons expressing cre recombinase from the *gad2* locus.

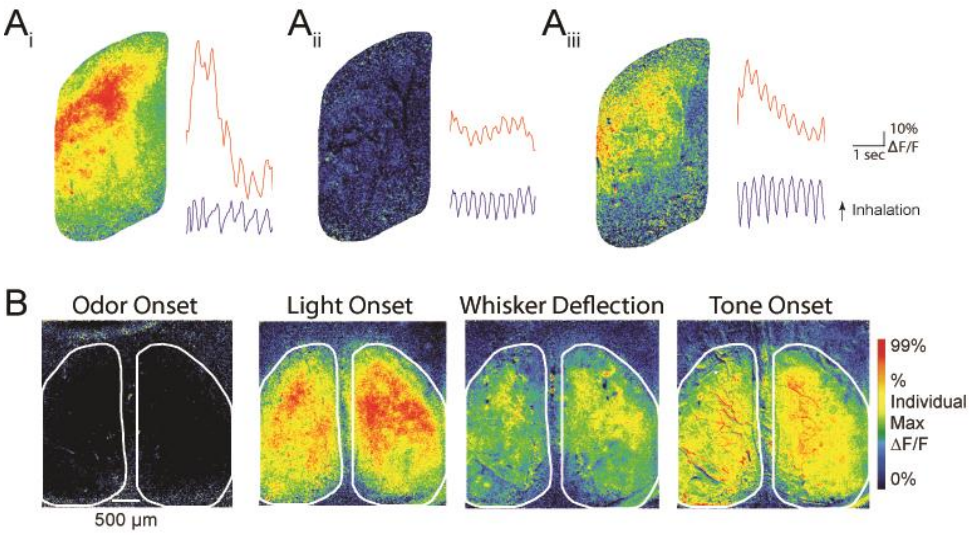

Figure 3. Cross-modal responses are not due to intranasal airflow*. A)* Representative pseudocolor maps with GCaMP3 fluorescence traces (red) along with thermocouple respiration traces (blue) in response to light onset. In some cases (Ai) respiration changes co-occur with changes in PG cell activity. Other instances show no changes in respiration with minimal to no alteration in PG cell activity (Aii), or no changes in respiration with large changes in PG cell activity (Aiii). *B*) Representative pseudocolor maps across stimuli after tracheotomy scaled to individual maxima.

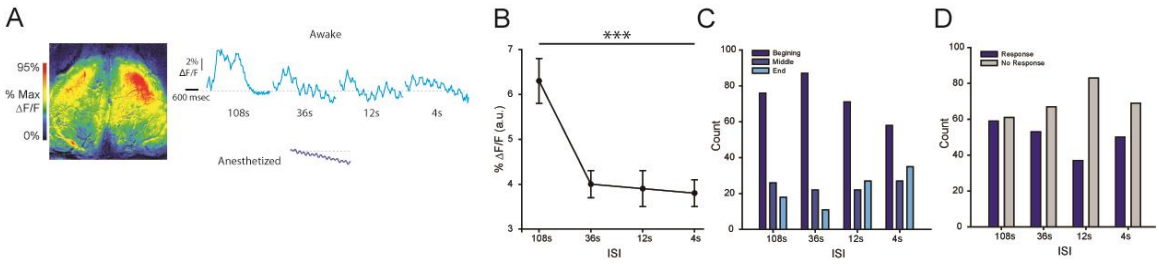

Figure 4. Non-olfactory responses decrease with decreasing inter-stimulus intervals. *A*) Pseudocolored light-evoked response map and example single trial traces of calcium signals in GAD65-PG cells (light blue) at 108-, 36-, 12-, and 4-sec ISIs in an awake animal. Analogous fluorescence trace in anesthetized animal (dark blue) for comparison. *B*) Average maximum whole bulb light-evoked response amplitude across ISIs (expressed mean ± SEM; 8 bulbs in 4 animals). *C*) Counts of temporal location of maximum light-evoked response amplitude across ISIs. Three second trials split into one second bins. *D*) Binarized count of light-evoked responses occurring (blue bars) or not occurring (gray bars) across ISIs.

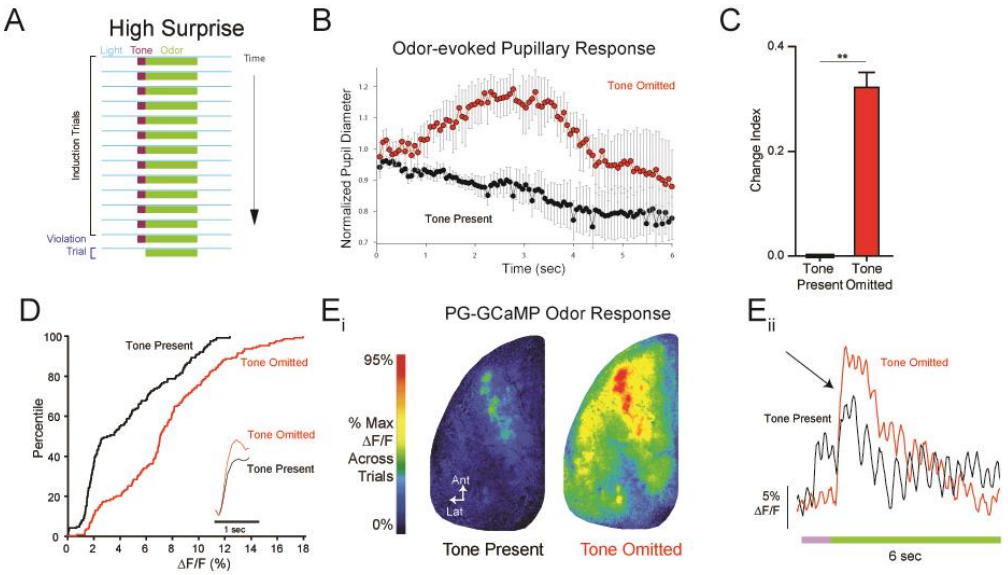

Figure 5. Expectation violation facilitates GABAergic signaling and suppresses presynaptic calcium in OSNs in the olfactory bulb. *A)* Paradigm schematic. *B*) Odor-evoked pupillary response shows pupil dilation on the tone omitted trial compared to the average of the previous three tone-present trials. *C&D*) Odorant-evoked intraglomerular GCaMP3 signals were significantly larger on first inhalation of tone omitted (red) trials than on preceding tone-present trials (black), as shown in Change Index (CI) (*C*; mean ± SE) and cumulative frequency distributions (*D*; average first sniff odorant-evoked fluorescence in inlay) across 137 glomeruli from 5 mice ** $p < 0.01$. *Ei*&*Eii*) Pseudocolor maps and fluorescence traces of odorant-evoked calcium signaling in GAD65-PG cell populations during tone-present (left/black) and tone-omitted (right/red) odorant presentations (green bar).

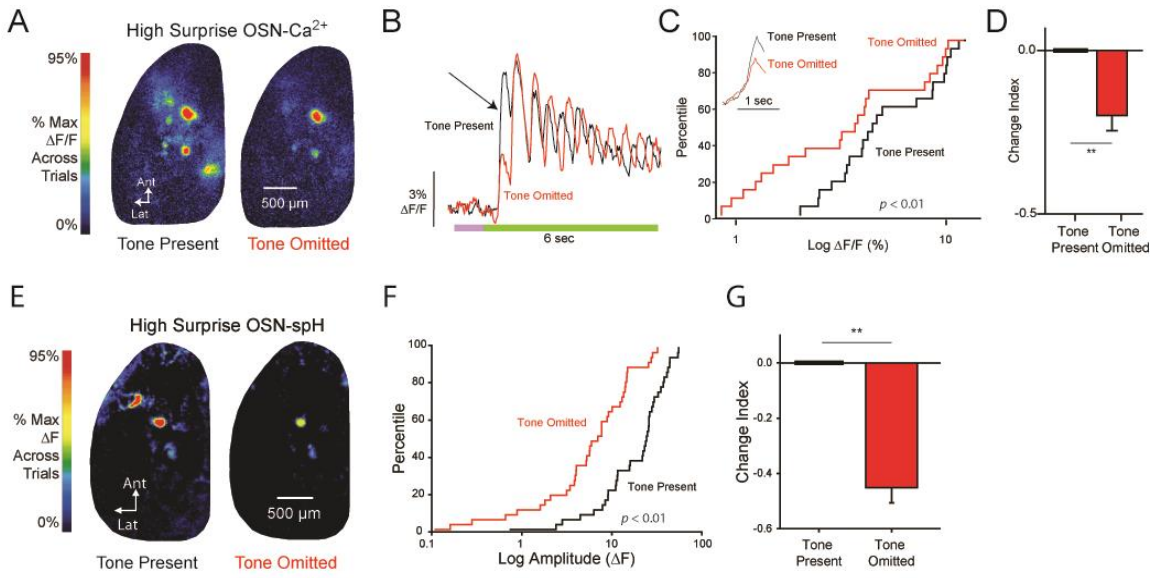

Figure 6. Expectation violation suppresses neurotransmitter release from OSNs*.* *A*) Pseudocolor maps of odorant-evoked fluorescence on last tone-present trial (left) and tone omitted trial (right) in OBs of an awake OMP-spH mouse. *B&C)* Odorant-evoked spH signals on tone-omitted (red) trials were significantly smaller than on preceding tone-present trials (black), as shown in cumulative frequency distributions (*B*) and Change Index (*C* across 38 glomeruli from 5 mice. ** $p < 0.01$ *D*) Representative pixel-by-pixel difference map of odorant-evoked fluorescence on last tone-present trial and following tone-omitted trial. Blue indicates suppression on tone-omitted trial. *E*) Odor-evoked pseudocolored maps as in A. *F)* Example fluorescence traces showing presynaptic calcium signaling in OSN terminals. *F&G*) Odorant-evoked intraglomerular Calcium Green signals were significantly smaller on first inhalation of tone omitted (red) trials than on preceding tone-present trials (black), as shown in cumulative frequency distribution. Average first sniff odorant-evoked fluorescence in inlay.

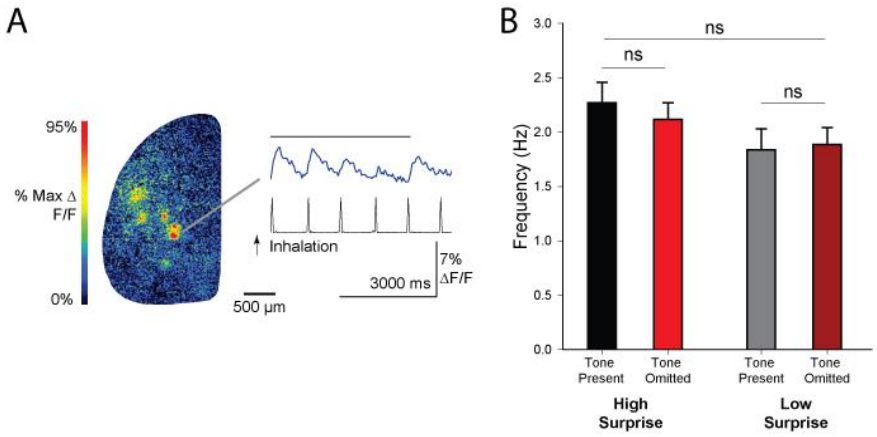

Figure 7. Expectation alters OSN response patterns without a change in odor sampling. *A)* Pseudocolor map and example fluorescence (blue, top) and respiration (black, lower) traces from an awake mouse during an odor presentation (black bar) showing that Calcium Green signal peaks phase-lock to inhalations. *B)* Summary data (mean ± SE) showing inhalation frequency (inferred from OSN-Calcium Green signal peaks) during the high and low surprise experiments. Mixed-model ANOVA revealed no change in sampling frequency between last tone-present trial and first tone-omitted trial.

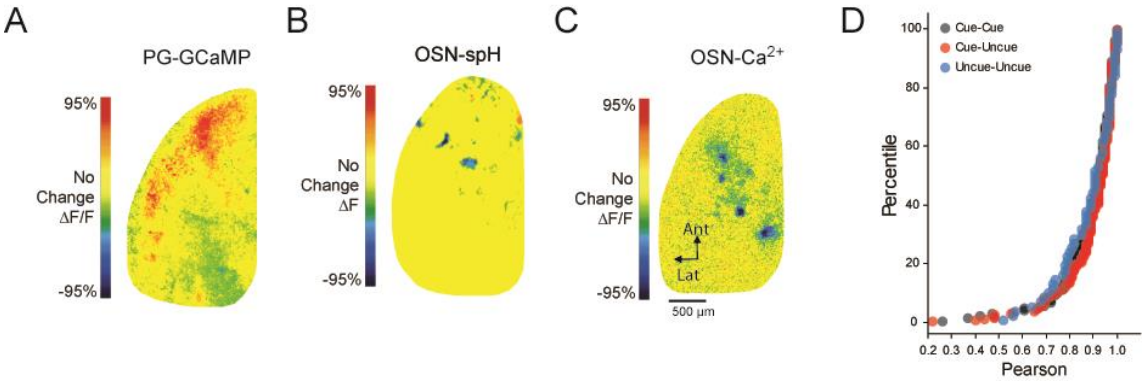

Figure 8. Tone omission does not change odor spatial representation. *A)* Representative pixel-by-pixel difference map of odorant-evoked signals on the first peak of the last tone-present trial and first tone-omitted trial. Red indicates increase on the tone-omitted trial. *B)* Representative pixel-by-pixel difference map of cumulative odorant-evoked spH signals of the last tone-present trial and the first tone-omitted trial. Blue indicates a decrease on the tone omitted-trial. *C)* Representative pixel-by-pixel difference maps of odorant-evoked Calcium Green signals on the first peak of the last tone-present trial and first tone-omitted trial. Blue indicates a decrease on the tone omitted trial. *D*) Correlations between glomerular response patterns between all possible two trial pairs. Correlations were coded as belonging to a tone present-tone present trial correlation (black), a tone present trial-tone omitted trial correlation (red), or a tone omitted-tone omitted trial correlation (blue). The distributions of Pearson rôs of each trial type combination were not different (Kruskal-Wallis, $p > 0.05$).

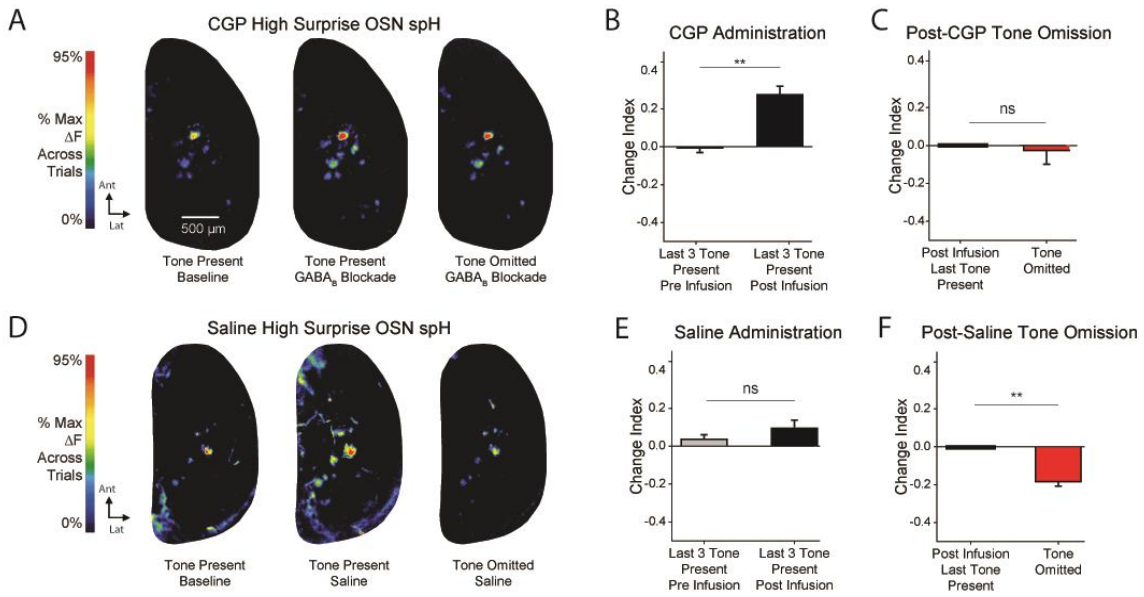

Figure 9. ***Expectation violation suppresses neurotransmitter release from OSNs via GABA$_B$ receptor-mediated presynaptic inhibition.*** *A&D*) Pseudocolor maps of odorant-evoked fluorescence on baseline tone-present trial, post-infusion tone-present trial, and post-infusion tone-omitted trial after $GABA_B$ antagonist or vehicle infusion. *B&C)* $GABA_B$ receptor blockade significantly enlarged odorant-evoked spH signals on last three tone present pre-infusion trials compared to last three tone present post-infusion trials (*B*; mean ± SE; 71 glomeruli from 4 mice). Vehicle infusion did not (*E;* 54 glomeruli from 5 mice). *C*) After $GABA_B$ receptor blockade, odorant-evoked spH signals on tone-omitted trials (red) were no different than preceding tone-present trials (black). *F*) After vehicle infusion, odorant-evoked spH signals on tone-omitted trial (red) were significantly smaller than on tone-present trials (black).

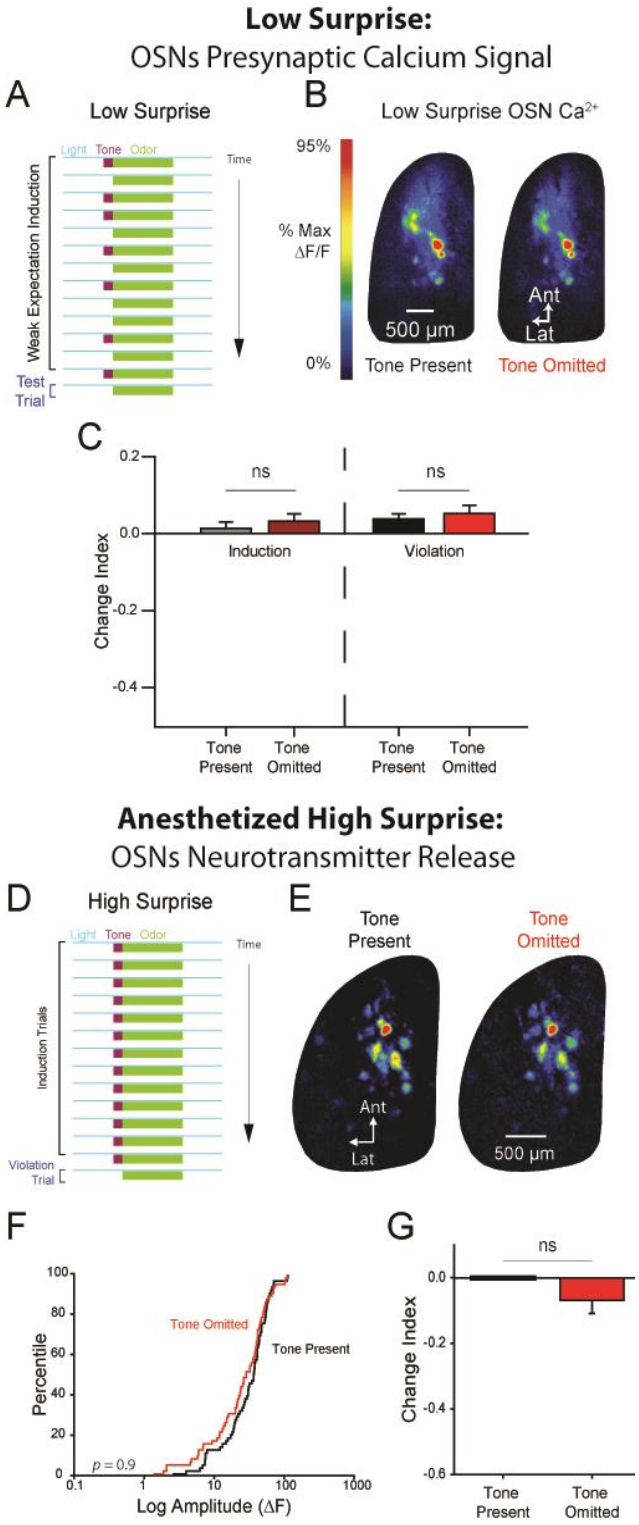

Figure 10. OSN suppression does not occur when tone omission is not surprising or when tone is omitted in anesthetized animals. *A*) Low surprise paradigm schematic. *B*) Pseudocolor maps of odorant-evoked fluorescence on the first sniff of the last tone present trial (left) and first tone omitted trial (right). *C*) No difference (mean ± SE, paired samples t-test) in response to odorant on tone-present and tone-omitted trials (Violation). During induction phase, average of last 3 tone-present (grey) and last 3 tone-omitted (dark red) trials was not different. *D*) High surprise paradigm. *E&G)* Analogous pseudocolor maps and CI measurements to *B* and *C* but in anesthetized OMP-spH mice. No difference in response amplitudes between the tone-omitted trial and preceding tone-present trial (*G*, mean ± SE, 60 glomeruli from 4 mice).

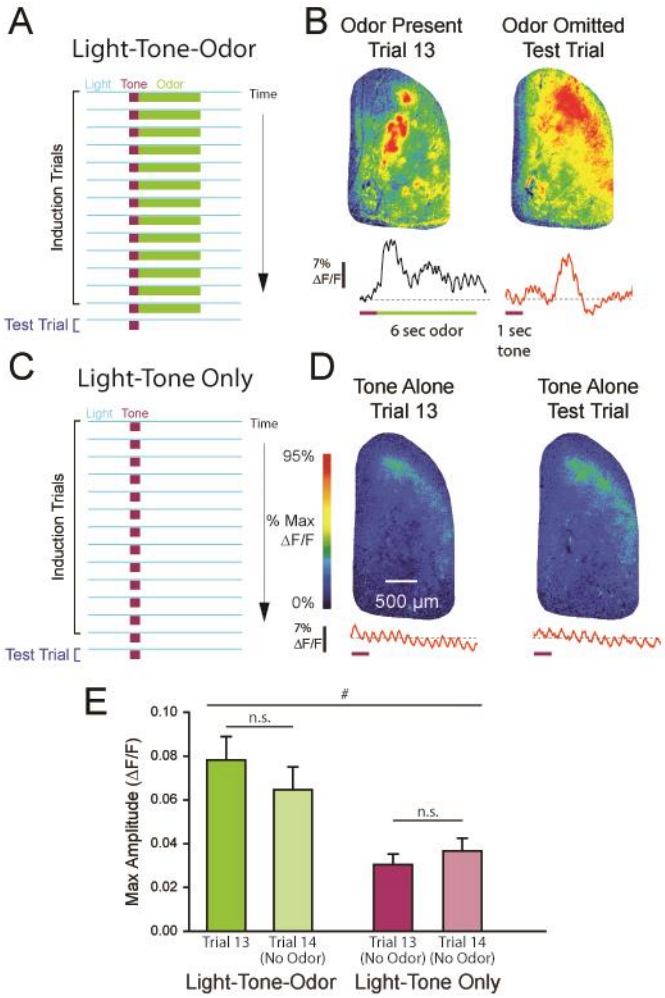

Figure 11. Expectation of odor presentation facilitates GABAergic signaling in the olfactory bulb. *A)* Paradigm schematic. *B)* Representative pseudocolor response maps of peak odor-evoked response on the final odor present trial, corresponding peak response on the following odor-omitted trial, and corresponding fluorescence traces. *C)* Control paradigm schematic. *D)* Pseudocolor response maps of peak response amplitude from the six seconds following tone presentation (corresponding to the odor presentation as in A) from the 13th and 14th trials (as in B) with corresponding fluorescence traces. *E)* Light-tone-odor GCaMP3 peak signals were significantly larger than corresponding peak responses in the light-tone only experiment (2 mice, mean ± SE; # $p < 0.02$). Response amplitudes were not significantly different between the 13th trial and 14th trial in either paradigm.

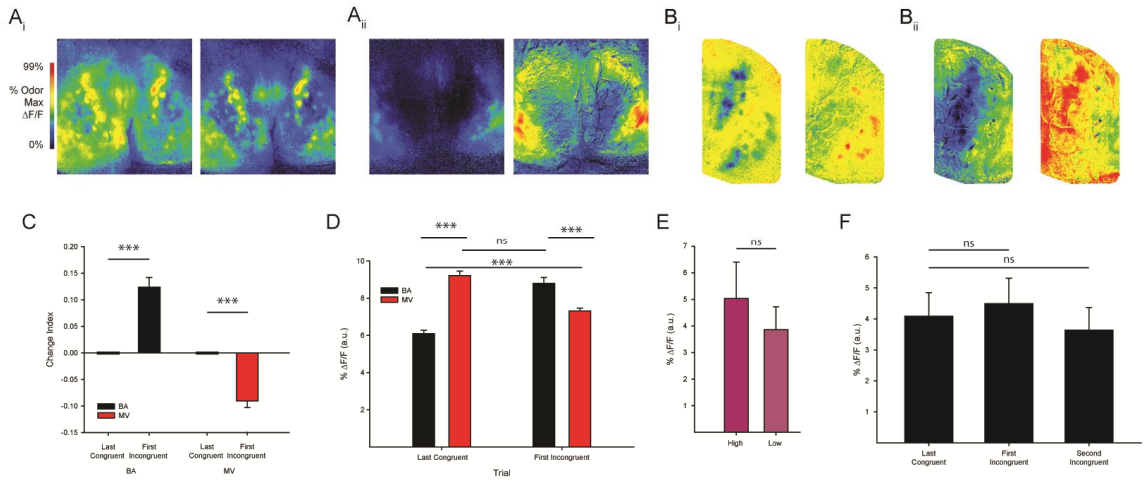

Figure 12. Simultaneous multimodal expectations impact odor coding. *A)* Pseucolored response maps of odor-evoked PG cell activity. *A_i)* GCaMP3 calcium transients evoked by methyl valerate (MV) when cued by MV-associated tone (left) or when cued by butyl acetate(BA)-associated tone (right). *A_{ii}*) GCaMP3 calcium transients evoked by BA when cued by BA-associated tone (left) or when cued by the MV-associated tone (right). *B_i)* Pseudocolored difference maps of odor evoked responses showing degree of BA tone suppression on MV (left) and degree of MV tone enhancement of BA (right). *Bi_i)* Difference map of BA tone congruent trial minus MV tone incongruent trial (left). Difference map of MV tone congruent trial minus BA tone incongruent trial (right). *C)* Average CIôs of the last BA (black) and MV (red) tone-congruent trials and first incongruent trials when tones are associated with the alternate odor (mean CI ± SEM; 671 glomeruli in 8 animals). *** $p < 0.001$ *D)* Raw odor-evoked response amplitudes (mean qF/F ± SEM) of MV (red) and BA (black) on last tone congruent trials and first tone incongruent trials. *** $p < 0.001$ *E)* Average maximal tone-evoked PG response amplitudes on the 13th trial of each tone frequency (mean qF/F ± SEM). *F)* Average raw maximal tone-evoked PG cell response on the last tone-odor congruent trial and first two tone-odor incongruent trials (mean qF/F ± SEM). Response amplitudes were not significantly different between trials.